UNIVERSIDADE DE LISBOA
FACULDADE DE CIÊNCIAS
DEPARTAMENTO DE FÍSICA

Development and Characterization of Lithium Formate EPR Dosimetry for Proton Radiation Therapy

Tatiana Pedro Cordeiro Costa

Mestrado Integrado em Engenharia Biomédica e Biofísica
Perfil em Biofísica Médica e Fisiologia dos Sistemas

Dissertação orientada por:
Prof. Doutor Luís Peralta
Prof. Emer. Eva Lund

2017

Nothing in life is to be feared, it is only to be understood.
Now is the time to understand more, so that we may fear less.

Marie Curie

ACKNOWLEDGMENTS

As my five-year journey as a MSc student ends, it is time to thank to everyone who guided and supported me throughout this process.

To my supervisors in Linköping, without who this work would not have been possible.

Eva Lund, thank you for always supporting and believing in me. You always showed such a big care, interest and high expectations for this work and your enthusiasm for EPR was certainly contagious and a great motivation! You are an inspiration as a person and as a professional for all the work that you have done and still do regarding the EPR research.

Emelie Adolfsson, you transmitted such a big confidence and feeling of easiness when you taught me all the first practical things about EPR. Thank you for always having your door open for my "basic" questions and though you haven't accompanied this work until the end I hope you are proud of it and of our results.

I hope I have represented well the EPR team and that this research is continued!

A big thank you to Skandion Clinic, especially to Marcus Fager and Alexandru Dasu. Your contribution was great and I cannot express my appreciation for the help and interest you showed in these experiments and for showing and explaining me all the practical details about proton therapy.

Também, não posso deixar de agradecer ao professor Luís Peralta por estar sempre disponível para me ajudar e responder às minhas dúvidas, mesmo não dominando por completo este tema. Sem qualquer dúvida, a exigência e rigor que o caracterizam ajudaram bastante a melhorar e a chegar a este meu trabalho final.

Ainda, um agradecimento à Reitoria da Universidade de Lisboa pelo apoio financeiro que, no âmbito do programa ERASMUS+, ajudaram à realização deste estágio.

Also, as this journey was much more than work, many other have to be mentioned.

To all my Linköping friends and to Karin Dahlgren for being my second family when I missed home the most. I don't think I could have gone through the cold and dark Swedish winter without you and all the good and fun moments we shared!

A todos os amigos que, mais longe ou mais perto, nunca me deixaram sentir só. Às minhas meninas de Leiria que já me acompanham há muitos anos e me conhecem melhor que ninguém e a aos amigos que ganhei na Universidade que verdadeiramente fizeram este caminho muito mais fácil.

Por último, não posso deixar de agradecer às pessoas mais importantes da minha vida. Pai, mãe e mano, obrigada por todos os votos de confiança que me deram - às vezes mesmo sem perceberem bem no que eu me estava a meter -, por me aturarem nos melhores e piores dias e, acima de tudo, por me apoiarem incondicionalmente em tudo. É a vocês que devo tudo e, por isso, um grande OBRIGADA!

RESUMO

A técnica de Ressonância Paramagnética Eletrónica, RPE (EPR do inglês Electron Paramagnetic Resonance) utiliza métodos de espectroscopia para a deteção de eletrões livres - ou radicais livres - em moléculas cuja estrutura cristalina permite a retenção e estabilização destes radicais. Os radicais livres formam-se, entre outras causas, devido à exposição das moléculas a radiação eletromagnética de energia considerável sendo a quantidade de radicais formados e retidos na molécula proporcional à dose de radiação absorvida por esta. Esta relação é o principio básico da RPE e diz-nos que através da contabilização dos radicais formados, por espectroscopia, é possível inferir acerca da dose radiativa absorvida por uma molécula, sendo este o principal objetivo da dosimetria.

Apesar da utilização da RPE para fins de dosimetria em radioterapia ser uma aplicação relativamente recente, trata-se de uma técnica já muito bem estabelecida em outras áreas. Em particular, a técnica RPE com dosímetros de alanina é mesmo recomendada pela Agência Internacional de Energia Atómica (IAEA do inglês International Atomic Energy Agency) não só para fins de dosimetria retrospetiva como também para a medição de doses de radiação superiores a 6 Gy.

As vantagens da utilização de alanina como material dosimétrico recaem na estabilidade dos seus radicais, na resposta linear num intervalo alargado de dose e no facto de ser um material cujas características de dispersão e absorção de radiação ionizante serem muito semelhantes às dos tecidos corporais. No entanto, apesar de todas as vantagens, a baixa sensibilidade da alanina não permite a sua utilização para a medição e verificação de doses inferiores a 6Gy, comummente utilizadas em tratamentos radioterapêuticos. Deste modo, foram estudados diversos materiais para encontrar o dosímetro mais adequado que, mantendo as características vantajosas da alanina, colmatasse o problema encontrado.

A melhor alternativa encontrada foi o formato de lítio que apresenta uma sensibilidade quase sete vezes superior à da alanina e uma maior equivalência à água no que respeita os coeficientes de absorção massa-energia em dose de radiação relevantes em tratamentos de radioterapia. Por conseguinte, o sistema de RPE com dosímetros de formato de lítio começou a ser considerado como uma melhor opção e diversos testes de caracterização têm vindo a ser realizados para aferir acerca da qualidade, estabilidade e adequabilidade desde novo sistema a várias aplicações em radioterapia.

O sistema em questão foi aplicado, com sucesso, para verificações dosimétricas em tratamentos de Radioterapia Externa como radioterapia de intensidade modulada (IMRT) ou radioterapia conformacional tridimensional (3D-CRT), em que doses de cerca de 2 Gy por dia – dependendo do plano de tratamento - são depositadas no tumor do paciente por um feixe de fotões produzidos num acelerador linear, e em tratamentos de Braquiterapia, em que radioisótopos são colocadas dentro ou próximo do alvo do tratamento. Em ambos os casos o sistema dosimétrico de formato de lítio mostrou

ser robusto, ter uma resposta linear às diferentes doses absorvidas e permitir determinações das doses com uma incerteza inferior a 2.5 %. Assim, mesmo não sendo uma técnica considerada para uso diário em clínicas, devido ao moroso processo de leitura do sinal de RPE, o sistema de dosimetria RPE de formato de lítio torna-se uma das mais vantajosas alternativas aos sistemas utilizados atualmente em aplicações em que a obtenção de medições de alta precisão é priorizada relativamente à eficácia de tempo, tendo já sido considerado um ótimo candidato para auditorias de dosimetria nas técnicas estudadas.

No entanto, apesar das elevadas expectativas, nenhuma investigação tinha sido ainda realizada relativamente ao funcionamento do sistema de formato de lítio após irradiação com partículas mais pesadas como protões, cujas interações com a matéria são consideravelmente diferentes das dos fotões.

Apesar do número de clínicas especializadas em terapia de protões ser relativamente reduzido devido aos elevados custos associados e, por conseguinte, a oferta deste tratamento ser ainda limitada, trata-se de uma alternativa à radioterapia convencional, com claras vantagens no que diz respeito à precisão e eficácia do tratamento que advêm principalmente da deposição de energia característica dos protões e do associado pico de Bragg, cuja profundidade de ocorrência é definida pela energia inicial dada às partículas. Os protões entram no novo meio com uma energia muito elevada e uma taxa de depositação de energia reduzida mas, com o aumento da profundidade e a diminuição da energia da partícula, esta taxa de deposição aumenta gradualmente, atingindo o seu máximo na profundidade do pico de Bragg, onde toda a restante energia das partículas é depositada e as partículas ficam em repouso, não depositando mais energia. Assim, controlando a profundidade do pico de Bragg, a maior dose pode ser depositada na área tumoral e os órgãos e tecidos envolventes podem ser poupados, evitando-se os danos colaterais associados à radioterapia convencional.

Deste modo, é de extrema importância a existência de um sistema de dosimetria de elevada qualidade que permita, com elevada precisão, a verificação das doses de radiação entregues pelos feixes de protões utilizados, devendo o sistema RPE ser considerado para esta aplicação.

O trabalho de investigação apresentado nesta dissertação foi realizado com o objetivo de aferir acerca das características do sistema RPE com formato de lítio após irradiações de protões e da influência que a diferente deposição de energia e interações destas partículas com a matéria podem ter no sistema em questão.

A investigação e consequente caracterização foi feita relativamente a dois tópicos principais: a taxa de resposta do sinal de RPE obtido pelos dosímetros aquando submetidos a doses de radiação entre os 0 Gy e os 9 Gy, através da obtenção e análise da curva Dose-Resposta do sistema, e do estudo do desvanecimento do sinal durante um período de um mês. Adicionalmente foi realizado um "teste cego" a fim de verificar a exatidão conseguida na estimação da dose absorvida por um dosímetro somente através do seu sinal RPE e da curva Dose-Resposta. Este trabalho de investigação foi realizado na Universidade de Linköping, na Suécia, em parceria com a recente clínica de terapia de protões Skandionkliniken, em Uppsala (Suécia), onde todas as irradiações de protões foram realizadas.

Os resultados confirmaram a elevada qualidade e precisão do sistema para verificações dosimétricas em terapia de protões.

A curva Dose-resposta mostrou uma relação linear entre o sinal de RPE dos dosímetros e a dose absorvida por estes pelo que um maior sinal corresponde a uma maior dose absorvida pelo respetivo dosímetro. A elevado valor do coeficiente de correlação de Pearson entre as variáveis foi interpretada como um forte indicador da qualidade das estimações que se obteriam através da relação encontrada e isto foi confirmado no teste às cegas em que, utilizando apenas dois grupos de dosímetros para determinar a curva de Dose-Resposta, a dose desconhecida fornecida a um terceiro grupo de dosímetros foi estimada com um erro de somente 1 %, apenas com base nos seus sinais de RPE e na regressão obtida.

Relativamente ao estudo do desvanecimento do sinal, cada grupo de dosímetros foi irradiado em semanas consecutivas durante um mês, tendo o sinal de RPE de todos os dosímetros sido medido no final desse mês, no mesmo dia. Os resultados foram evidentes: os sinais de RPE dos dosímetros cujas irradiações decorreram nas primeiras semanas da experiência sofreram um desvanecimento maior, tendo sido registado um desvanecimento máximo na ordem dos 6.50 % durante o período de tempo estudado. Este fenómeno, que não havia sido verificado nos sinais de dosímetros sujeitos a radiação de fotões, constitui assim um dos mais importantes fatores a ter em conta aquando da utilização do sistema para verificações dosimétricas neste tipo de irradiações com feixes de protões.

Após os testes efetuados, é possível afirmar que o sistema de dosimetria RPE com formato de lítio mostrou ser robusto e bastante eficaz em verificações dosimétricas também nesta aplicação. No entanto, e apesar de uma análise mais extensa deste fenómeno ser necessária, foi comprovado o desvanecimento do sinal de RPE com o tempo pelo que o intervalo de tempo decorrido entre a irradiação e a leitura do sinal do dosímetro se torna num elemento preponderante e determinante na medição de doses absorvidas com a maior precisão possível.

Assim, apesar de poderem ser necessárias algumas correções aos sinais obtidos no espectrómetro, quando a leitura destes sinais não é imediata à irradiação, o potencial deste sistema é inquestionável, devendo o sistema RPE com formato de lítio ser visto como um forte candidato a ser usado, por exemplo, em auditorias de dosimetria em terapia de protões.

Palavras-chave: Ressonância Paramagnética Eletrónica
Formato de Lítio
Terapia de Protões
Curvas Dose-Resposta
Desvanecimento do Sinal

ABSTRACT

Electron Paramagnetic Resonance (EPR) dosimetry using lithium formate dosimeters started to be studied as an alternative to the well-established dosimetry method that uses alanine as dosimeter material, so that a higher precision and accuracy in the measurements of low absorbed doses commonly used in radiation therapy could be achieved.

Lithium formate has shown to be a material with properties very similar to alanine and thus very suitable for EPR dosimetry, but with the advantage of being up to seven times more sensitive to smaller radiation doses. The proposed dosimetry system was tested in both external beam therapy (photon therapy) and in brachytherapy and the system showed to be very robust, allowed dose determinations with a standard uncertainty lower than 2.5 % and was considered a good candidate for dosimetry audits in both radiotherapy modalities.

The next step and the aim of the present dissertation work is the study and characterization of the lithium formate system under proton beam irradiations. The use of heavy charged particles is associated to very different interactions of the energy with matter and, consequently, to different dose deposition processes that may influence the dosimetry system performance. So, despite the suitability of the system for the other clinical applications, no assumptions can be made about the system quality for dose measurements in proton therapy.

In this way, the system was studied regarding two main characteristics: the dose response and the phenomenon of signal fading. This research work was mainly based in Linköping University (Sweden) but it involved a partnership with Skandionkliniken in Uppsala (Sweden) to perform the necessary proton irradiations.

The first test studied the relation between the EPR signals and the absorbed dose and the results showed that not only the obtained regression that characterizes that relation is, as expected, linear but also allowed absorbed dose to water estimations with an average estimation uncertainty below the 2 %. To complement this test and to verify what accuracy could be reached with a linear regression estimated with only two groups of dosimeters, a group of four dosimeters was irradiated with an unknown dose that was further estimated with an error of 1 %, confirming the great determinations that can be achieved with the present dosimetry system.

The second study indicated that, after proton irradiations, the EPR signal stored in the lithium formate dosimeters decreases with time and, for a period of 31 days, a maximum fading of 6.50 % was discovered. This phenomenon is not unexpected in irradiations with heavy particle beams and needs to be considered if the irradiation and the EPR signal measurement are not done in the same day because

if a smaller signal than the one associated to the real absorbed dose is considered, erroneous conclusions will be consequently taken regarding the absorbed dose by the dosimeter.

Overall, though more studies need to be done, especially regarding the fading associated to the dosimeters EPR signals, the lithium formate dosimetry system is considered a very promising tool for dose verifications in proton beam irradiations. The system not only presents a linear behaviour as it allows dose estimations with uncertainties lower than the 4 % uncertainty limit accepted in dose delivery processes. Therefore, the lithium formate dosimetry system might actually be a good candidate for audits in proton radiation therapy.

Key-words: Electron Paramagnetic Resonance (EPR) dosimetry

Lithium Formate

Proton therapy

Dose Response

Signal Fading

TABLE OF CONTENTS

LIST OF FIGURES

LIST OF TABLES

ACRONYMS

3D-CRT	Three-dimensional Conformal Radiotherapy
CT	Computer Tomography
EPR	Electron Paramagnetic Resonance
IAEA	International Atomic Energy Agency
ICF	Individual Calibration Factor
ICRU	International Commission on Radiation Units and Measurements
IMRT	Intensity Modulated Radiation Therapy
ISS	Istituto Superiore de Sanità
LET	Linear Energy Transfer
LIU	Linköping University
OAR	Organ at Risk
PMMA	Polymethyl Methacrylate
SSD	Source-Surface Distance
TLD	Thermoluminescence Dosimeter
VMAT	Volumetric Modulated Arc Therapy
WHO	World Health Organization

Chapter 1

INTRODUCTION

Cancer is one of the leading causes of morbidity and mortality worldwide. This group of diseases is characterized by an uncontrolled growth and spread of cells, which can invade various parts of the body and other organs, and affects around 14 million people every year, being responsible for about 8 million deaths per year according to the World Cancer Report [1] from the World Health Organization (WHO).

Each of the over one hundred different types of cancer require unique diagnosis and specific treatments that must be planned by specialized oncologic teams. Radiation therapy, or radiotherapy, together with surgery and chemotherapy are the three main modalities used for cancer treatment.

Radiotherapy as the procedure of using ionising radiation for cancer treatment can be divided into two main groups: external beam radiotherapy and brachytherapy. In the first, the radiation source is at a certain distance from the patient and the target is irradiated with an external radiation beam while in brachytherapy the radiation sources are placed close or even inside the target volume [2].

The use of ionising radiation for medical purposes has been a topic of study and concern for many years now. The effectiveness of this treatment modality is related with the sensitivity that cells have to radiation and how this radiation can damage the genes, interrupting the cell cycle and, consequently, leading to the death of cells. The main problem is that, regardless of its efficacy in killing the cancerous cells, the ionising radiation also affects normal tissues and damage them, which originates the severe side effects associated to most radiotherapy treatments like sore skin, tiredness or hair loss, among many others. Consequently, all over the world, specialists and researchers work on the development of new methods and solutions to reach the best balance between destroying cancer cells and minimizing damages to the surrounding healthy tissues.

When not considering the influence of the type of cancer and its degree of development, the effectiveness of a treatment depends mainly on two factors: the accuracy of the treatment planning and the quality of the equipment and technologies of the radiation systems available.

Concerning the treatment planning process, the dose distributions of target volumes and critical organs are assessed for each patient and the optimal technique among the treatment modalities available is chosen by qualified professionals. The planning process starts with the obtainment of a 3D image of the patient, most commonly a Computed Tomography (CT), so that the most accurate and realistic data regarding the anatomy of the patient and the tumour characteristics (location and volume) are used. This data is then used as the input for the planning software that contours the different volumes encountered.

Accounting this, a specialized medical physicist identifies both the tumour volumes and the surrounding tissues and Organs at Risk (OAR) and defines the necessary dose distributions.

A team of physicists together with radiotherapy doctors work to set the final details of the plan and, in the end, if every step of the planning process is successfully and accurately done, the best and less harmful treatment for each individual situation is obtained.

Besides having a precise treatment plan with all the structures well-defined and bordered it is of the greatest importance that the dose delivery system is also working as expected so that the delivered dose matches the planned one.

Medical physicists working with radiotherapy have the responsibility to verify that the correct dose is being delivered in the right direction towards the patient by performing regular quality controls and, with this, make sure that the tinny margin that separates the treatment efficacy and the occurrence of severe side effects is not exceeded.

The ideal dose is defined as [3]:

> "The ideal radiation with which to treat cancer is one that
>
> delivers a defined dose distribution within a target volume."

All radiotherapy procedures as susceptible to errors and even the smallest errors during the treatment planning, the dose delivery process or in the dosimetry verifications may cause substantial negative consequences for the patient. Considering this, it has been argued that the accuracy of the dose delivery to the patient in a radiotherapy treatment should be better than 3-4 % [4], considering all the possible inaccuracies associated to radiotherapy beam characteristics, patient data, treatment planning dose calculations and absorbed dose determinations.

In order to accomplish the accuracy and precision needed, radiation dosimetry or, more specifically, medical radiation dosimetry, becomes an essential part of the treatment control.

Medical radiation dosimetry consists on the evaluation, through measurement or calculation, of the absorbed dose received by a patient that is exposed to ionising radiation as a consequence of therapeutic or diagnostic procedures [5]. Nowadays, there are several methods and equipment available for dose verification measurements and each has different characteristics so, according to the aim of the measurement, the most suitable and convenient method should be used.

Radiation detectors may be divided in two main groups according to how the signal read is displayed. Using a direct reading detector, such as ionization chambers or semiconducting diodes, the signal is displayed instantaneously whereas using passive detectors like thermoluminescent detectors (TLD) or Electron Paramagnetic Resonance (EPR) detectors the effects caused by ionizing radiation result in data that has to be processed to obtain the signal information regarding the radiation [6].

The first group of detectors are, therefore, preferred for clinical applications because they can show the result much fast way. In fact, historically, ion chambers have been the main choice for the measurement of the absorbed dose in beams of ionising radiation and most dosimetry protocols are based on the use of ionization chamber since it is one of the most accurate and well-known method for dose determinations [7]. Though, passive detectors are usually characterized by a lower dependence on the direction of the beam, do not require connecting cables – a factor that sometimes makes impossible the use of ionization chambers -, and are associated to very precise measurements so, in some circumstances, passive detectors can become the most suitable equipment to be used.

The present thesis is focused on the EPR technique. Its use in radiation therapy is a relatively new advance but EPR spectroscopy is already a well-established technique for other dosimetry applications. In fact, the EPR spectroscopy technique using alanine as the dosimeter material has been accepted and recommended by the International Atomic Energy Agency (IAEA) mostly for retrospective dosimetry [8] and, concerning radiotherapeutic purposes, for the measurement of doses of

radiation over the 6 Gy [9]. However, the low sensitivity of most EPR materials used so far made it very difficult to achieve the precision recommended by the International Commission on Radiation Units and Measurements (ICRU) at the dose levels administrated in radiotherapy.

The dose determination using the EPR technique is rather time consuming so it is not the most suitable technique to be used on the daily basis in clinics and, additionally, requires the purchase and use of an expensive high precision spectrometer. Nonetheless, this technique gains relevance due to the accuracy that might be reached if more sensitive dosimeter materials are used and because of the possibility of repeating the measurements several times without influencing the radiation signal, allowing the increase of the results certainty.

So, in applications that prioritize the achievement of a high precision and accuracy and do not require a time efficiency, EPR dosimetry with more suitable and sensitive dosimetry materials, become a very realistic and advantageous alternative to other dosimetry systems.

Research was made to find more appropriate materials for this purpose and one of the most promising materials is polycrystalline lithium formate monohydrate, commonly referred as lithium formate. The EPR dosimetry system with this material has already been tested for dosimetry purposes in some radiotherapy techniques like external beam therapy and brachytherapy and the conclusions were very pleasing.

Under high LET (Linear Energy Transfer) radiation, however, the behaviour of the system was still not studied and for the technique to gain status and consideration among the other dosimetry techniques used in radiotherapy, the full characterization of the lithium formate EPR dosimetry system under every type of radiation is needed. Particularly, due to the promising benefits of proton therapy upcoming its high precision dose delivery, the search for accurate and well-known systems for dose verifications is becoming more and more important.

1.1. AIM

The present project is focused on the continuation of the characterization of the promising lithium formate EPR system for dose measurements under clinical proton beams.

The alternative of using lithium formate instead of alanine is thought to be considerably more beneficial for dose verifications because it is argued to have such a great accuracy that it can measure absorbed doses down to 0.2 Gy, accordingly to previous research. In this way, when low uncertainty dosimetry methods are needed and the high precision is preferred over the time efficiency, the EPR dosimetry method may be considered as the most suitable one in comparison with ionization chamber dosimetry or thermoluminescence dosimetry, for example.

The lithium formate EPR system has been developed, tested and optimised for photon beams and was considered a good candidate for dosimetry audits in both external beam therapy and brachytherapy. However, the different characteristics of photon beam therapy and charged particle therapy result in different radiation-matter interactions and in different dose distribution over the target. Consequently, the behaviour of a dosimetry system is expected to have some differences.

Considering these differences, the greater need to have accurate dosimetry systems for dose verifications in proton beams and the promising results obtained for photon beam dose verifications, the lithium formate EPR dosimetry must also be fully characterized for proton beam irradiations. This is where the present project is inserted.

A lithium formate EPR dosimetry system was developed and tested for proton beams with the aim of being characterized regarding the linearity of its response to different doses and also study the stability of the signal read on the dosimeters over a period of one month.

All the process of the dosimeters production, calibrations, EPR signal readouts and respective analysis were performed in Linköping University (LiU). The proton irradiations needed for the study of the lithium formate dosimeters response were done in the new Swedish proton therapy facility in Uppsala, Skandionkliniken.

1.2. OUTLINE

Chapter 2 provides a literature review over the EPR technique and the present state of the use of this dosimetry system for radiation therapy dosimetry controls.

Chapter 3 describes the types of radiation used for radiotherapy purposes: photon therapy used in the conventional radiotherapy and particle therapy where the proton therapy is inserted.
The main interactions of the ionising particles with matter are clarified and the main characteristics of the proton radiation therapy are enhanced.

Chapter 4 clarifies the main concepts of radiation dosimetry. The most important quantities in dosimetry used for the quantification of radiation are explained as well as the most important terms used in Radiation Protection and in Medical Dosimetry. Also, a section regarding radiation dosimeters contains the description and principal characteristics of the most commonly used systems with special focus on the Electron Paramagnetic Resonance technique.

Chapter 5 presents the materials and methodology used in each experiment. This section includes the description of the manufacture of the lithium formate dosimeters, the homogeneity test and standards needed for a batch to be considered homogeneous, the EPR readout procedure and the methodology followed for the Linearity Test, Blind Test and Fading Test.

Chapter 6 presents the results obtained in each experiment. The analysis is firstly focused on the acceptance of the batch as homogenous or non-homogeneous and, secondly, focused on the results of the main tests where statistical analysis is also presented. Finally, the obtained results are discussed and compared to previous research made regarding the EPR dosimetry and the use of lithium formate dosimeters.

Chapter 7 gives general conclusions regarding all the tests made and the lithium formate dosimetry system behaviour. Also, future directions are given.

Chapter 2

LITERATURE REVIEW

Since the early 20th century, radiation therapy has been used for the treatment of cancer. However, medical dosimetry is a relatively new field and, particularly over the past 40 years, the concept as changed a lot and, nowadays, is seen as an essential part of quality assurance in medicine all around the world [10].

The medical physics main goal to increase the accuracy and precision of the dose delivery justifies a current research in several fields related to medical dosimetry and, for this reason, a big focus is on the passive dosimeters since most of them are characterized by long term stability, wide dosimetric range, small dimensions and the lack of cables or power supplies [11].

To understand the EPR technique principles is important to go back to the 1920s, where scientists began to apply quantum mechanics principles to describe atoms and molecules. From the Stern-Gerlach experiments was possible to conclude that an electron magnetic moment in an atom can only take discrete orientations under the influence of a magnetic field and that atoms can absorb energy and orientate themselves according to the frequency of the radiation they are exposed to. As a result of this and many other quantum physics discoveries, the first observation of an EPR peak was registered in 1945 by Zavoisky when he detected a radiofrequency absorption line from a $CuCl_2 2H_2O$ sample.

In 1962, Bradshaw [12] demonstrated that EPR was a satisfactory technique for the measurement of radiation doses since the amplitude of the obtained absorption line was directly related with the dose itself. He suggested the use of a polycrystalline sample of the amino acid α-alanine as detector material (dosimeter) due several of this material features like:

- **high sensitivity to radiation damage**: large amounts of free radicals are created in the alanine structure after irradiation

- **stability:** the radical population formed is stable in time, making the dosimeter signal virtually independent of the time of irradiation

- **similarity to biological systems in absorbing radiation**: the atomic composition of alanine is tissue or water equivalent to that of human tissue

In the consequent years, EPR dosimetry has developed in a way that allowed it to be accepted as a competitive method at higher dose ranges (10 to 10^5 Gy) to other dosimetry methods [13].

Moreover, in the beginning of the 1980s, IAEA chose alanine as the standard dosimetric material for high dose measurements due to its particular and well-known characteristics [14].

At the Istituto Superiore de Sanità (ISS) in Italy, the method of manufacturing solid state alanine dosimeters was set up in 1983 and the same method was patented in 1985. There, the physicists made a big analysis regarding the response of the dosimeters to gamma rays and the main results were coherent with previous experiments: dosimeters with very precise and with reproducible results, no substantial energy or dose rate dependence neither influence of the angle in which the dosimeters detect the radiation beam [15].

After this, alanine EPR was established as a precise and accurate dosimetric method likely to be applied not only in industrial radiation processing but in radiation therapy as well.

Despite the advantages associated to alanine dosimeters like their tissue-equivalence and requiring no energy correction within the range of typical therapeutic beams, their sensitivity was not good enough for them to be used in clinical applications that require determinations of lower doses, ranging from 0.2 to 5 Gy [16]. So, aiming to make EPR a competitive dosimetry method for medical applications, research was made to find more sensitive materials for EPR dosimeters.

In 2002, polycrystalline lithium formate monohydrate, commonly known as lithium formate, was confirmed to have a sensitivity up to seven times higher than alanine [17] and so, dosimeters made from this material started being analysed with the thought that they could have some clear and practical advantages over alanine dosimeters. The advantages of using lithium formate as dosimeter materials were enhanced in a later study [18] where was shown that these dosimeters allow the measurement of absorbed doses down to 0.2 Gy. Consequently, they were considerable suitable to measure the lower dose ranges that could not be measured by the alanine dosimeters and, additionally, their linear response to all ranges indicated promising results for the measurements of doses both in the target of radiotherapy procedures as in the surrounding areas.

For intensity-modulated radiation therapy (IMRT), three-dimensional conformal radiotherapy (3D-CRT) and volumetric modulated arc therapy (VMAT), the lithium formate EPR dosimetry was tested and compared with the ionization chamber [19]. The determined doses agreed very well with planned doses and with the doses measured by ionization chambers confirming the potential of this dosimetry technique in terms of accuracy and the reproducibility of the measurements in external beam therapy with photons. Concerning dose measurements around brachytherapy sources with photon energies relevant to this technique, the referred EPR system also showed very accurate results [20, 21].

For irradiations with proton beams, the radical formation in lithium formate dosimeters was studied and reported [22]. In this research, the doses given were between 5 and 20 Gy and conclusions showed that the EPR reading signal increased linearly with the dose given and the precision of the reading was high and comparable with the precision obtained in previous studies of lithium formate using photon and electron beams.

At the same time, as the LET increased the relative effectiveness of the irradiation - defined as the dosimeter signal per absorbed dose in the detector - decreased and this decrease was interpreted as the result of several interactions and recombination within the tracks of the high LET particles. With this study the indication that the radical population trapped in the lithium formate structure after irradiation with densely ionising radiation is less stable than irradiation after low LET beams was clear and the importance of a study regarding the whole lithium formate dosimeter characterization especially with high LET particles was more enhanced. The lower stability of radicals after high LET radiation exposures had been previously referred in a publication from 1989 [23] where the signal from alanine radicals faded over the time.

Though the research regarding lithium formate EPR is quite promising, many studies are still focusing in alanine EPR technique since it is the standard dosimetry method. In 2015, research showed

the suitability to use alanine EPR technique for dosimetry characterization of proton beams with range between 10 Gy and 70 Gy [24]. Yet, not much more has been done regarding the characterization of the system, particularly to lower radiation doses justifying the need and adequacy of the present project.

The viability of any dosimetry system using for dose verifications in therapy is primarily verified with dosimetry audits where the same technique is tested in several clinics [25]. The great performance of an audit for clinical trials is what assures the dosimetry accuracy among the different participating clinics and is what warrants reproducible treatment protocols.

In the present days, EPR dosimetry using alanine has already been used for audits in the United Kingdom, Italy and Belgium. These audits enhanced the possibility to use alanine detectors to verify the dosimetry accuracy of conventional photon and electron beams [26]. Additionally, an end-to-end test using alanine dosimetry was designed and tested showing that alanine dosimeters are also suitable detectors for audits in heavy particle therapies. However, in this same work some of the weaknesses of the alanine dosimeters were exposed, in particular the lower sensitivity to lower doses.

Considering lithium EPR dosimetry, in Linköping University (Sweden), an audit system for high energy external beam therapy using lithium formate dosimeters was also developed [27] with the aim of evaluating the behaviour of these dosimeters during the whole treatment chain (end-to-end test) including CT imaging, planning and dose delivery. To get more realistic results, a head to neck phantom made of Polymethyl Methacrylate **(**PMMA**)** with heterogeneities was designed and built and the system was tested in four clinics in Sweden. Results showed that the developed audit system was suitable for end-to-end audits since all the measured dose values agreed quite well with the calculated doses enhancing, once again, the great characteristics of the used dosimetry system.

Chapter 3

RADIATION IN RADIOTHERAPY

Radiation therapy consists on the use of ionizing radiation to treat a disease, most likely cancer. The concept of ionizing radiation includes any electromagnetic or particle radiation with enough energy to ionize common molecules and create electrically charged particles – ions – with the liberation of one or several electrons [28].

The ionizations can occur directly once the particle radiation interacts with the matter or the interaction might initiate nuclear or elementary-particle transformations that, by their turn, result in ionization. So, ionizing radiation can be divided in directly and indirectly ionizing radiation.

Directly ionizing radiation includes several types of charged particles such as electrons, protons, alpha particles or heavy ions and means that these particles transfer most of their kinetic energy directly to the medium resulting in absorbed dose by the medium. Indirectly ionizing radiation, on the other hand, means that the energy is imparted to matter in two steps: firstly, the indirectly ionizing radiation transfers energy as kinetic energy to secondary particles and only then these charged particles transfer most of their kinetic energy to the medium, resulting in the absorbed dose. In this last type of radiation are included neutral particles like photons and neutrons.

For medical purposes is also possible to distinguish two types of radiation used in radiotherapy treatments: photon radiation and particle radiation, which will be described next. The basis of radiotherapy, whatever type is considered, is the way the ionizing radiation and matter interact with each other and the expected effects of radiation in tumorous cells are always a consequence of the transfer of energy of the charged particles moving through a medium to the atoms of the body cells.

3.1. PHOTON RADIATION

Under the modern theory of light, presented by Albert Einstein in the beginning of the 20th century, a photon is a *quantum* of electromagnetic radiation. In radiotherapy, the most common beams used are high energy x-rays and gamma rays, generically named as photon beams. However, the electromagnetic spectrum also includes radio waves, infrared rays, visible light and ultraviolet rays and

all these consist of photons so when referring to photon beams is important to specify what type of radiation is being used.

What differs among the several radiation types is the photons energy (E) that is known to be proportional to the photons frequency f.

$$E = hf \quad \text{(Equation 3.1)}$$

The relation between the variables is given by Equation 3.1 where h is the Planck's constant[1].

$$f = \frac{c}{\lambda} \quad \text{(Equation 3.2)}$$

Since the frequency of the electromagnetic radiation and its wavelength λ can be related by Equation 3.2, where c represents the speed of electromagnetic-field propagation, Equation 3.1 can be rewritten so that the photon energy can be calculated only considering the wavelength λ of the radiation.

$$E = \frac{hc}{\lambda} \quad \text{(Equation 3.3)}$$

Therefore, the energy of each photon, given by Equation 3.3, does not depend on the intensity of the radiation since they all contain the exact same amount of energy. The intensity of a beam is a function of the number of photons striking a given surface area per unit time.

Most external radiation therapy is delivered through linear accelerators – *linac* - where electrons are accelerated to very high velocities and led to strike a heavy metal target to create a beam of photons. When moving through materials they are likely to interact with the matter in different ways, producing different ionizing photon radiations.

The most important interactions [6] to consider in radiotherapy include:

- **Photoelectric effect**

This effect is the consequence of the interaction between the electromagnetic radiation and the atoms from an attenuator, usually a metal. When the energy of the photons is higher than the electrons' binding energy, all their energy is transferred to the orbital electron that is ejected from the attenuator with a kinetic energy equivalent to the photon energy minus the binding energy. The empty spot left by the ejected electron is then filled by an electron from an upper orbital, resulting in the emission of characteristic X-rays or in the ejection of Auger electrons.

The probability of this effect depends on several factors and among those factors are the photons energy and the atomic number of the material that absorbs the radiation. For example, for materials with high atomic number, the photoelectric is considerable for higher energies but for materials or compounds with low atomic number (like water) the photoelectric effect is not likely to occur at energies over 200 keV.

- **Compton scattering**

Represents the interaction of an energetic photon with a quasi-free orbital electron. The incident photon energy has to be considerably higher than the binding energy of the orbital electron and, with the interaction, the photon transfers part of its energy to the electron and is scattered in a different direction with a higher wavelength.

[1] Constant that relates de energy in one quantum (photon) of electromagnetic radiation to the frequency of that radiation. The value of this constant is approximately 6.626 x 10^{-34} J.s

The energy given to the electron is, of course, dependant on the initial photon energy and the angle of scattering: a scattering angle closer to 180° results in a larger amount of energy to the electron which is scattered approximately in the photons original path. On the other hand, a small scattering angle corresponds to a smaller amount of energy given to the electron. After the photon-electron interaction, the photon with a lower energy may continue undergoing additional interactions.

The angular distribution of the photons scattered is given by the Klein-Nishina cross section that is independent of the atomic number of the material and that is why it is quite difficulty to distinguish tissues in medical images when these images are obtained with energies where the Compton scattering dominates: between 25 keV and 25 MeV. In this range are included the energy levels used in most radiation treatments and so, the Compton scattering is one of the most important interactions in radiotherapy with photon radiation.

- **Pair production**

Originated by the interaction of a photon with the nucleus of an atom and not their orbital electrons, the pair production refers to the creation of an electron-positron pair. In this context, the photon disappears and an electron-positron pair is produced in the nuclear Coulomb field.

The new particles move away with the remaining energy of the photon converted to kinetic energy. Since mass is produced out of the photon energy, the pair production effect has an energy threshold of $2m_e c^2 = 1.02\ MeV$. The two will typically be annihilated once they lose their kinetic energy, originating annihilation radiation (characteristically photons with 0.511 keV).

The probability for it to happen is proportional to the logarithm of the incoming photon energy and is dependent on the atomic number of the material it goes through. The energy in which pair production dominates is above the 25 MeV in water.

All the above interactions influence the total attenuation of the photon beam in a medium and have to be considered to obtain a more exact quantification of the photon absorption and scattering. The contribution of each interaction to the beam attenuation in water is represented in Figure 3.1.

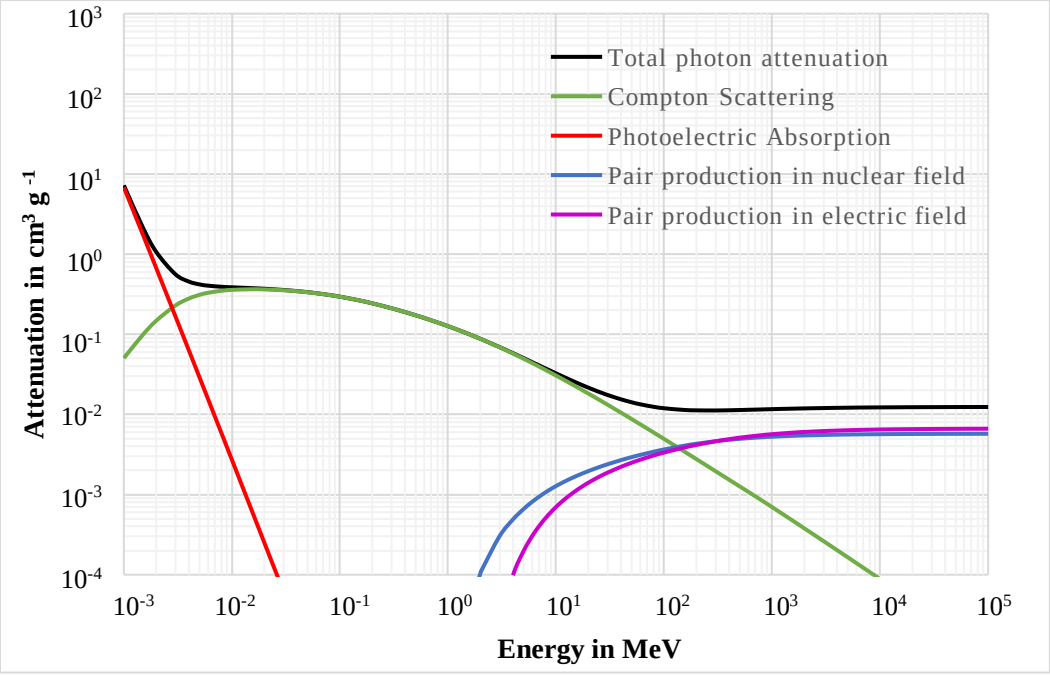

Figure 3.1 - Contribution of each type of interaction to the total photon beam attenuation in water. All interactions must be considered in order to calculate accurately, in the treatment planning, the radiation dose that the body will receive and therefore the dose that will be absorbed by the different body tissues.

In a radiotherapy treatment, the photons used produce a cascade of interactions before the energy is absorbed as dose, both in the treatment machine and in the patient body. These interactions, that might be either one of the above mentioned, where the energy is transferred from the photons to (secondary) electrons and positrons occur as soon as the photons interact with the material atoms. So, characteristically, the peak dose of photon beams is reached within a few millimetres from the entrance point – "build-up effect" -, at a depth correspondent to the range of the first secondary electrons produced. The new energetic particles will then ionize and excite other atoms until the initial energy transferred to them is lost or the particles exit the body. The beam energy is controlled so that the peak dose occurs after a few millimetres from the entrance point and the skin is saved from the radiation.

Another important characteristic is the low-LET that X-rays and Gamma rays are characterized for. LET, the acronym for Linear Energy Transfer, is a term applied to quantify energy transferred per unit length of the track. So, being classified as low-LET means that the radiation penetrates tissues very easily but deposits its energy very infrequently.

Each accelerated photon causes only one ionization that releases one electron but the secondary electrons produced cause many more ionisations and produce other energetic electrons along their track. The LET from gamma radiation depends on the energy of those secondary electrons.

As less energy is transferred from the photon to the target and more is conserved in the photons, they can travel further and the probability of interactions with other particles from the medium (including healthy surrounding tissues) increases. The typical dose deposition from two different photon beams is represented in Figure 3.2 by the blue and red lines.

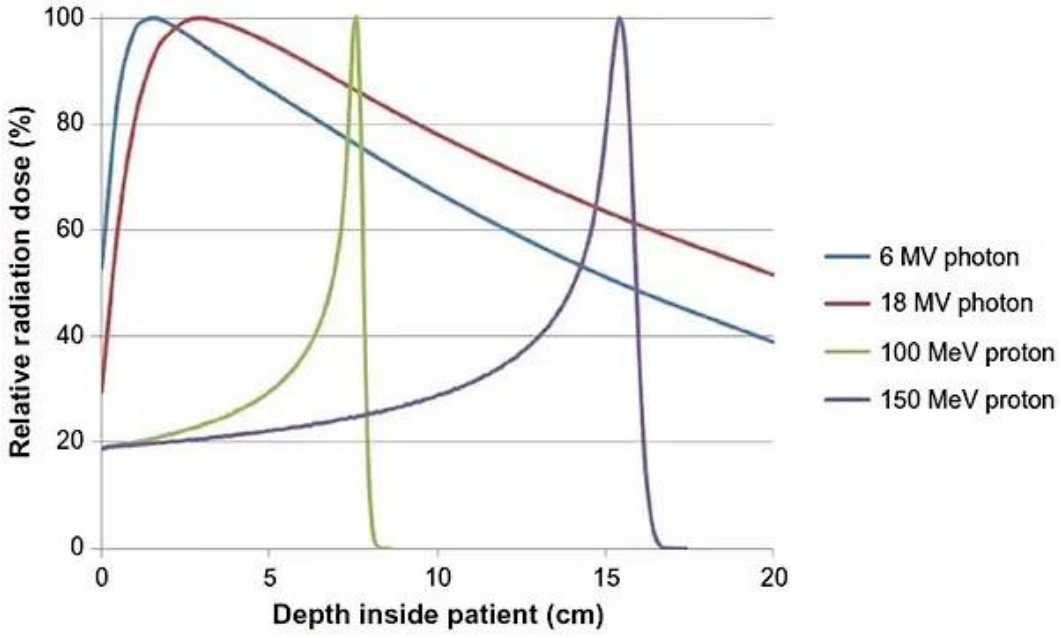

Figure 3.2 - Dose deposition as a function of depth within the body: comparison between photon beams and a proton beams. Photons deposit radiation dose as they penetrate through the body what results in photon beams irradiating healthy tissues in the whole path. On the other hand, with a proton beam, the largest amount of energy is deposited at a defined depth called Bragg Peak and in the rest of the path tissues only absorb relatively small doses of radiation. *[52]*

To control the dose that is deposited in each tissue, the solution passes by the use of several radiation beams delivered from different angles. Nowadays a commonly used technique for this is intensity modulated radiotherapy (IMRT) because it also allows a better dose conformation. This high precision 3D technique uses a computer-driven machine that moves around the patient and, in each of the pre-defined angles, delivers precise radiation doses, that can vary from angle to angle. With

knowledge of the tumour shape and its characteristics and after the medical team identifies the area to treat and the maximum dose that can be absorbed by the organs at risk, the best dose intensity pattern that best conforms to the tumour is determined by a medical physicist.

The combinations of various intensity-modulated fields from different directions allows the delivery of a higher dose to the tumour and, at the same time, limits the amount of radiation that is deposited in the healthy tissues that are on the beam path.

Despite all the improvements in treatment technologies such as multi-leaf collimators, IMRT or image-guided radiotherapy (IGRT), photon beam therapy is always be responsible for healthy tissues to receive considerable radiation doses resulting in harmful side effects for the patient undergoing the treatment. Like so, alternative treatments in which these effects are smaller must be considered.

3.2. PARTICLE RADIATION

This group includes not only hadrons as protons and heavy ions but also neutrons and electrons, all considered ionizing particles for radiotherapy purposes.

The interest in using charged hadrons is related with the existence of the denominated Bragg peak which increases the ability to optimise the spatial distribution of the absorbed dose within a tissue and makes particle radiation the best and more advantageous choice for many cancer treatments.

The Bragg peak indicates the point of greatest penetration in the tissue and it occurs because the stopping power of the particles increases right before they come to rest. It represents the maximum depth the particles reach and this depth is determined by the amount of energy that is given initially to the particles by the accelerator. So, the Bragg peak depth can be controlled by the physicist aiming to a very precise targeting of the tumour tissue. The particles enter the new medium with a very high energy and begin to deposit very small radiation doses that increase gradually with the depth increase and the particle energy reduction. When the Bragg peak depth is reached, the particles deposit their remaining energy and stop irradiating immediately after.

The Bragg curve is a graph of the energy loss rate of ionizing radiation as a function of the distance through a stopping medium. This curve is also represented in Figure 3.2 where the dose deposition of protons is compared with the dose deposition of photon radiation and the differences between both techniques are enhanced.

Contrarily to what happens with photon radiation, where the dose deposition peak is reached within a few millimetres from the entrance point of the photon beam, in the particle radiation case, most energy is deposited at the depth of the Bragg peak, after which the dose rapidly decreases to zero and all particles come to rest if no nuclear reactions occur and secondary neutral particles are created.

This property reduces significantly the exposition of healthy surrounding tissues to radiation so, in theory, this reduction of toxicity will also reduce the probability of developing secondary malignant tumours induced by the radiation that appear some years after the radiotherapy treatments, a risk that appears to be higher for survivors of childhood cancers [29]. In this way, the tolerance of the patients to the treatment is higher as well as their life quality during and after the treatment.

Besides the advantages related to the Bragg peak that optimise the absorbed dose delivered to the target, there are other reasons behind the great interest in the use of particle radiation in radiotherapy. These reasons are based both on the physics of the dose transport and deposition and on the radiobiological effects they have.

The large mass of charged hadrons results a minimal degree of multiple scatter allowing a well-defined lateral definition of the beam.

Another advantage of hadrons is their high LET when the interaction with the tissues occur. By the definition of LET, high LET radiation causes more molecular damages per unit of exposure because large amounts of energy are deposited in small distances. So, the higher localised deposition of energy results in a greater relative biological effectiveness (RBE) associated to the use of hadrons in comparison with the photon radiation whose secondary electrons are characterised by a low LET. Also, since tumours are characterised for being hypoxic[2] which makes them more resistant to radiation, the oxygen enhancement ratio (OER) of hadrons becomes a considerably important attribute of hadrons.

Due to all the potential advantages of particle radiation in radiotherapy that is associated with a more effective treatment and less harmful consequences for the patient, a higher attention is being given to the use of proton and other charged particles like helium or carbon ions.

In the present context, a special focus is given to proton therapy [5].

3.2.1. PROTON THERAPY

Proton therapy is an emerging treatment modality to treat cancer and its concept arises from 1946 [30] after Robert Wilson described some physical properties of protons and hypothesised that high energetic proton beams could be used to increase the radiation doses to tumours and, at the same time, minimize radiation to nearby healthy tissues.

The first treatments using heavy ion beams with protons were performed in 1954 [31] at the Harvard Cyclotron Laboratory and due to the lack of many clinical conditions (treatment planning, beam shaping technology,) were only suited for radiosurgery like pituitary ablation.

In Europe, the first synchrocyclotron was developed in Uppsala University (Sweden) around 1950 by Borje Larsson and there, in 1957, it started to be used for cranial radiosurgery and fractionated radiotherapy [32].

Regardless of the excellent records about the treatment safety and efficacy, the widespread and adoption of this technique is being quite slow mostly because of its technical difficulty, much higher costs of implementation and the lack of evidence of cost-competitiveness. Yet, this technique has grown quite a lot and in 2015 there were 51 active proton therapy centres all over the world, 16 of those in Europe [33]. So, in the future is expected a big spread of proton therapy facilities which will make this technique a more approachable alternative to conventional radiotherapy.

The technique, as the name indicates is based on the use of protons that are accelerated to really high velocities and can be used for therapeutic purposes. Protons are positively charged and heavy particles (in comparison with electrons) and their biggest advantage is the way the destructive power is delivered to the tissues associated due to the characteristically high LET. Also, protons travel fast through tissues with few interactions and without changing much the original trajectory until they reach a defined depth where the Bragg peak occurs and the dose is deposited.

The high dose distribution given by the proton beam to the tumour, with minimal or no exit dose, allows the tumour to be treated with unmatched accuracy, security and efficiency. By sparing healthy surrounding tissues, the characteristic side effects of radiotherapy are significantly reduced and the life quality of the patient during and after the treatment is much better.

For a realistic treatment plan and, thus, a safe treatment is important to be aware of the interactions that protons may have with the matter since these interactions is what determine how the dose will be distributed, how much will be absorbed by tissues and allow to predict how much energy losses during the beam path.

[2] Privation of adequate oxygen levels at the tissue level

Protons interact with matter and deposit their energy in mostly in three different ways: energy loss by ionization, multiple Coulomb scattering and nuclear interactions. The first two interactions concern the electromagnetic interaction between the charge of a proton and the charge of atomic electrons - or the Coulomb field of the nucleus - whereas the third regards the interaction with the material nucleus.

- **Energy Loss by Ionization**

At the energy levels used clinically, the collisions of protons with atomic electrons, named inelastic Coulomb interactions [34], have a considerable importance.

As the protons mass is about 1800 times greater than the mass of electrons [35], each interaction can only reduce the proton energy a little but since the number of interactions is high, these interactions are the main reason for the slowdown of protons in matter and eventually their stopping after the proton range is reached.

The quantum theory of slowing down and stopping process was developed by Bethe and Bloch in the 1930s and predicts the rate of energy loss as a function of the type and energy of the incident particle and of the composition of the stopping material [36].

The energy loss per unit distance is called stopping power (S) [37] and is defined in Equation 3.4, where E is the energy and x refers to the distance protons go through. The unit for S is MeV/cm.

$$S = -\frac{dE}{dx} \quad \text{(Equation 3.4)}$$

Since the stopping power is proportional to the density of the absorbing material, this rate is usually expressed as a quantity independent of its mass density ρ (g/cm^3), being called mass stopping power. This quantity is expressed in $MeV.cm^2/g$ and given by Equation 3.5.

$$\frac{S}{\rho} = -\frac{1}{\rho}\frac{dE}{dx} \quad \text{(Equation 3.5)}$$

Apart from the interaction of charged particles with atoms and molecules being a statistical process, the energy loss occurs as a finite number of individual interactions so it has a statistical error associated. This means that protons with the same initial energy will probably not stop at the exact same depth due to the accumulation of several small variations during the energy loss - range straggling [35]. Though this process is only responsible for a fluctuation of about 1 % in the protons range [36], it can have quite an influence in the Bragg curve shape so it has to be considered if a precise clinical calculation is needed. This precision is of vital interest in radiotherapy because the main advantage of using charged particles is their precise dose deposition in a specific point.

- **Multiple Coulomb Scattering**

In addition to the possible interactions with atomic electrons that result in some energy loss, when passing near an atomic nucleus protons experience an elastic Coulomb scattering caused by the charge of the nucleus and are deviated through small angles from their original trajectory. Elastic and inelastic Coulomb interactions are designated as Multiple Coulomb Scattering [34].

The energy loss can be neglected in this process but the changes in the trajectory of protons, even the smaller ones, may be of the utmost importance and must be considered in the optimization of dose delivery.

The distribution of the angles after multiple scattering is nearly Gaussian and the Multiple Coulomb Scattering theory proposed by Goudsmit-Saunderson predicts with great accuracy the width of that Gaussian. The characteristics of the multiple scattering angle are predicted as a function of the incident particle type and energy and the composition of the scattering material [35, 36].

- **Nuclear Interactions**

Protons can also interact with the nucleus itself via some non-elastic reactions and these might have a much more profound effect in the fate of an individual proton. In these nuclear interactions, the nucleus is irreversibly transformed because when a proton is absorbed, the nucleus produces energetic secondary protons, deuterons, some other heavier ions or one or more neutrons. Protons and neutrons are the most important secondary particles to consider because they carry away energy far from the point where they are created.

The main effect of nuclear reactions within the therapeutic region of a proton field is a small decrease in absorbed dose due to the removal of primary protons. However, this decrease is mostly compensated by the release of secondary protons and other ions. Secondary protons energy corresponds to about 10 % of the absorbed energy in high energy proton beam treatments so they have small but sill non-negligible impact on the dose spatial distribution in a patient [37]. The other ions formed comprise only about 1 % or less of the therapeutic absorbed dose.

Similar to what is done for photon beams, in the proton beam treatment planning all the possible interactions that protons have with the medium must be considered and calculations must be done so that the absorbed dose is predicted as accurately as possible. In Figure 3.3 is illustrated a Monte Carlo simulation of the planar integrated dose distribution of a proton beam in water and the importance of each interactions for the total dose is clear.

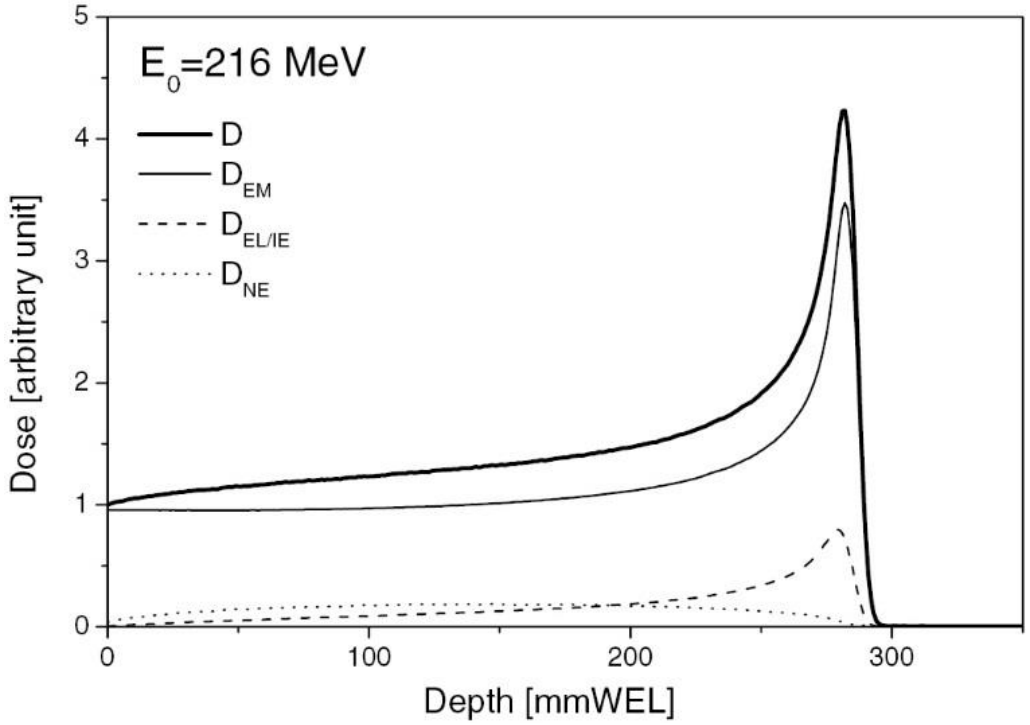

Figure 3.3 – Monte Carlo simulation of the planar integrated dose distribution of a proton beam in water. The dose from the electromagnetic interactions (D_{EM}) has the bigger influence since they are the biggest reason for the deceleration and stop of proton The dose resulting from scattered protons ($D_{EL/IE}$) also is considered as well as the dose from nonelastic nuclear (D_{NE}) that has a much smaller influence but still has to be considered in the calculations. *[49]*

Though they can be predicted, neither of the interactions cannot be avoided and some result in undesirable effects during a proton beam therapy. One of the most important is actually the production of a small dose of high energetic neutrons during the treatment resulting, for example from the interaction of the accelerated protons on the beam production and delivery equipment [37]. Even with the existence of a shielding against neutron radiation in any proton therapy installation, the neutron production cannot be avoided because they are also produced in the patient itself.

Neutrons are known for having a strong biological effect so even minor neutrons doses might actually have a great impact in the induction of secondary malignancies regarding the long term health of cancer patients.

The long term effects of proton therapy is one of the most controversial topics regarding this technique because the use of proton therapy as a real alternative to the conventional radiotherapy is a relatively new advance and, though the neutron production also happens during the photon beam therapy, the relative impact of it in each technique is still not certain. However, studies comparing secondary malignancies between patients treated with proton beams and photon beams show a smaller incidence of these side effects for proton therapy: 5.2 % of proton beam therapy patients had some secondary malignancies in comparison with 7.5 % of photon beam patients [38]. Despite this is a controversial issue, research is being made to study the adverse effects of proton therapy and it appears that the risk of adverse side effects associated with this technique is still lower than the risks in conventional radiotherapy.

Nowadays, proton beam therapy advantages are more evident and its importance is being more and more recognized by the medical community. Though, each cancer has its own characteristics as well as the many possibilities of treatments which means that, depending on the situation, some therapies are more adequate than others.

Proton therapy is the option of excellence when the treatment options are limited (e.g.: inoperable tumours) and the conventional therapy using photon beam presents unacceptable risks to patients, like when the tumours are localized in close proximity to vital organs: central nervous system tumours, ocular tumours, head and neck tumours, chest tumours, gastrointestinal tumours and pelvic tumours. Another very common use of proton therapy is in the treatment of paediatric tumours mostly because by avoiding the exposure of high levels of radiation to normal tissue when they are still developing stage, cognitive impairments, growth defects and cardiac damages can be prevented, as well as radiation induced tumours and other morbidities in the consequent years.

Chapter 4

RADIATION DOSIMETRY

The exposure to low levels of ionising radiation is a part of everyone's day since radiation is naturally present in the environment and, at low levels, causes no adverse health problems. However, at higher levels, like the ones used in medical treatments, ionising radiation can be dangerous if preventing and controlling measures are not adopted.

At higher levels, radiation is responsible for cell death and that is why it is used for radiotherapy purposes. However, in these treatments, radiation affects not only the cancerous cells but also the healthy tissues around and for a controlled and effective treatment, besides knowing the intrinsic characteristics of the type of radiation used, it is essential to accurately quantify the radiation dose to deliver to the tissues. Like so, radiation dosimetry plays an essential role in any radiotherapy procedure.

Radiation dosimetry is the subject that describes methods for the quantitative determination of energy deposited in a medium by ionizing radiation and, more importantly, the dose absorbed by the tissues. Consequently, radiation physicists are the responsible ones for finding the best balance between the purpose of the application and the negatives consequences of the exposure.

4.1. Dosimetry Quantities

The final aim of medical radiation dosimetry is to know how much radiation is absorbed by the different tissues in the body when they are irradiated. For this reason, the quantity we aim to determine in the most accurate and precise way is the absorbed dose that will be further explained.

To measure the absorbed dose from ionising radiation the knowledge of some dosimetry quantities beforehand is essential [6].

4.1.1. Fluence

A radiation field can be described either by the number of particles existing in the field – particle fluence – or by the energy that those particles transport – energy fluence.

The particle fluence Φ is defined by Equation 4.1 and refers to the number of particles d*N* that pass through a sphere with cross-sectional area d*A*. The particle fluence is independent on the incidence angle of the radiation so the incident radiation and the cross-section area are always perpendicular. The unit of fluence is m^{-2}.

$$\Phi = \frac{dN}{dA} \quad \text{(Equation 4.1)}$$

From the particle fluence equation is possible to obtain the energy fluence ψ, or the total incident energy that passes through the sphere with cross-sectional area d*A*, by knowing the energy *E* carried by each particle. The energy fluence is defined by Equation 4.2 and has the unit of J m^{-2}.

$$\psi = \left(\frac{dN}{dA}\right) E = \Phi \mathrm{E} \quad \text{(Equation 4.2)}$$

4.1.2. ENERGY IMPARTED

This term is defined by the total amount of ionizing radiation to matter in a volume.

As expressed in Equation 4.3, it results of the sum of the energies of all charged and uncharged ionizing particles that enter the volume R_{in} and the sum $\sum Q$ of all changes of the rest mass of nuclei and other elementary particles resulting from any interactions in the volume, less the sum of the energies of all charged and uncharged particles that leave the volume R_{out}. The energy imparted unit is Joule (J).

$$\varepsilon = R_{in} - R_{out} + \Sigma Q \quad \text{(Equation 4.3)}$$

4.1.3. KERMA

Regarding the ionization of uncharged particles, is also possible to define kerma (kinetic energy released per unit mass). Kerma quantifies the average amount of energy transferred from the uncharged ionizing particles $d\bar{E}_{tr}$ to charged ionizing particles per unit mass d*m*.

Kerma, defined in Equation 4.4, is expressed in J/kg or gray (Gy).

$$K = \frac{d\bar{E}_{tr}}{dm} \quad \text{(Equation 4.4)}$$

Though kerma is quite relevant for indirectly ionizing radiation, the location and the amount of energy that is transferred to the ionizing particles are not indicators of the energy that will be absorbed by the particles in the medium because not all ionizing particles interact with matter.

4.1.4. CEMA

Cema, as the acronym of converted energy per unit mass, is the analogue to kerma but applicable to directly ionizing particles such as electrons and protons. This quantity describes the energy E_C lost in electronic interactions by the charged particles, with exception of secondary electrons, with a mass d*m* of a material, as expressed in Equation 4.5. Similarly to kerma, the SI unit is also gray (Gy).

$$C = \frac{dE_C}{dm} \quad \text{(Equation 4.5)}$$

4.1.5. ABSORBED DOSE

The most important quantity for radiological protection refers to the amount of energy that is absorbed by the biological material. The absorbed dose is defined by Equation 4.6 and represents the quotient of mean energy imparted $d\bar{\varepsilon}$ by ionizing radiation to an infinitesimally small volume of mass *dm*. This quantity is relevant to both directly and indirectly ionizing radiation and its SI unit is also Gy.

$$D = \frac{d\bar{\varepsilon}}{dm} \qquad \text{(Equation 4.6)}$$

The process of dose deposition has a stochastic nature and so the interactions with matter are not continuous and the atoms with which the charged particles interact and are quite random. So, the absorbed dose is calculated as the mean of this stochastic distribution of energy in a volume element.

4.2. RADIATION PROTECTION QUANTITIES

The basic physical quantity in dosimetry is, as mentioned, the absorbed dose but for the radiation protection evaluation this quantity is not enough mostly because it does not represent entirely the effectiveness in damaging specific human tissues or organs.

Each type of ionizing radiation has different effects on body tissues that might be more or less resistant to that radiation. Consequently, the intrinsic properties of the tissues/ organs must also be considered when planning a treatment and evaluating the amount of radiation that should be given.

4.2.1. ORGAN DOSE

The amount of radiation dose absorbed by each organ can be defined by Equation 4.7. The organ dose results from the quotient between the total energy imparted ε_T to that tissue or organ and the mass m_T of that same organ/ tissue. As the other mentioned doses, the SI units is Gy.

$$D_T = \frac{\varepsilon_T}{m_T} \qquad \text{(Equation 4.7)}$$

4.2.1. EQUIVALENT DOSE

The mean absorbed dose in an organ or tissue has a clear importance in radiation protection but, by itself, is not enough to assess the biological damages to that organ. The dose distribution within an organ has also to be considered and so, information about the radiation type and energy is needed.

With energetic photon radiation, for example, each ionization event is more spaced from the others and is associated with less energy contrasting the ionization events produced by heavy particle radiation where much more energy is deposited in each event (high LET) and the events occur much more closely. So, logically, the radiation weighting factor w_R for photons must be lower.

The equivalent dose given to an organ or tissue T in then given by Equation 4.8.

$$H_T = \Sigma\, w_R D_{T,R} \qquad \text{(Equation 4.8)}$$

The multiplication between the radiation weighting factor w_R and the organ dose associated to one type of radiation gives the equivalent dose of that specific radiation type. However, in a treatment an organ can be irradiated with more than one type of radiation, so all contributors to the dose must be considered. The total equivalent dose H_T results of the sum of products of each w_R and $D_{T,R}$.

The values of w_R, selected by the International Commission on Radiological Protection (ICRP) and revised in 2007 [39] are:

- 1 for photons and electrons
- 2 for protons
- 20 for α-particles and heavy ions
- 2.5 – 20 for neutrons, depending on the neutron energy E_n and according with the continuous function:

$$\begin{cases} 2.5 + 18.2\, e^{-[\ln (E_n)]^2/6}, & E_n < 1MeV \\ 5.0 + 17.0\, e^{-[\ln (2\,E_n)]^2/6}, & 1\,MeV \leq E_n \leq 50\,MeV \\ 2.5 + 3.25\, e^{-[\ln (0.04\,E_n)]^2/6}, & E_n > 50\,MeV \end{cases}$$

The unit for the equivalent dose given by J/kg but takes the special name of Sievert (Sv).

4.2.2. EFFECTIVE DOSE

Besides considering a factor associated to each type of radiation, also a tissue weighting factor w_T must be considered because the radiobiological effects also depend on the organ or tissue irradiated.

The tissue weighting factors must represent the relative contribution of each organ to the total detriment due to the effects of a uniform irradiation of the whole body. For this reason, the quantity effective dose E, expressed in Equation 4.9 and with SI unit of Sievert, as to be considered.

$$E = \Sigma\, w_T H_T \qquad \text{(Equation 4.9)}$$

The effective dose is the weighted average of the mean absorbed dose to the several body organs and tissue, each with their respective w_T, and exposed to an equivalent dose H_T. The values for w_T have been defined by the ICRP in publication 103 [39] and are tabulated in IAEA safety standards and are applicable to the average population, despite of the sex and age of the person. For example:

- 0.01 for bone surface, brain, salivary glands and skin
- 0.05 for the bladder, liver, oesophagus and thyroid
- 0.08 for gonads
- 0.12 for breast, lungs, red bone morrow, colon and stomach

4.3. RADIATION DOSIMETERS

The radiation doses are measured with specific detectors: radiation dosimeters.

A dosimeter along with its reader is referred to as a dosimetry system [6] and every dosimetry system can be characterised by:

- **Precision**

High precision is associated with a small standard deviation of the distribution of the several measurement results. Under similar conditions the measurement results must be reproducible and accurately predicted from previous measurements.

- **Accuracy**

Accurate results are similar to the 'true value' of the measured quantity which means that the radiation dose detected by the dosimeter must be coherent with the planned delivered dose by the radiation beam.

The difference between these two, or the inaccuracy of the result, is called the uncertainty of the measurement.

- **Dose or dose-rate dependence**

The response of the dosimetry system must be independent of the rate of the dosimetric quantity measured. However, high dose rates usually influence the dosimeter readings, leading to the saturation of the system.

- **Energy Dependence**

Most dosimetry systems are calibrated at a quantified radiation beam quality but are used in a much wider energy range. It is known that the response of the dosimetry system is usually a function of the radiation beam quality so the energy dependence of a dosimetry system must be known to allow necessary corrections. Ideally the energy dependence of a system should be as low as possible.

- **Spatial Resolution**

Dosimeters should allow the determination of radiation dose from a very small volume because is important that the dose can be characterized at every point of the tissue.

Radiation detectors can be divided in two groups according to whether the signal is displayed instantaneously or not and presently, for the daily use in clinic environments, techniques that display the result faster and accurately are preferred. Ionization chamber dosimetry is the most commonly used dosimetry technique for dose verifications and beam calibrations but, as mentioned, in some cases this technique is not suitable to be used.

Other dosimetry systems to consider are film dosimetry, luminescence dosimetry, diode dosimetry and, important to refer in the context of the present dissertation, Electron Paramagnetic Resonance Dosimetry. Each one of these dosimetry techniques have their own characteristics, advantages and disadvantages and so, the dosimeter system choice must take into account the requirements of the measurement situation so that the most suitable system is chosen.

This thesis is focused on EPR technique as a viable alternative to the existing dosimetry systems. Though it can be seen as an alternative to ionization chamber dosimetry in some specific situations, the main application of this technique is thought to be dosimetry auditing. In this field, luminescence dosimetry is a technique that is very well established and to which EPR dosimetry should be compared with.

To know the general characteristics, advantages and disadvantages of the dosimetry systems mentioned, the ionization chamber dosimetry and thermoluminescence are now summarized and a bigger attention and description is given regarding EPR spectroscopy for dosimetry purposes.

4.3.1. IONIZATION CHAMBER DOSIMETRY

The ionization chamber is nowadays the most practical and most used type of dosimetry used for dose control and measurements in radiotherapy.

Apart from the different appearances the device may have, it always consists in a gas filled cavity surrounded by a conductive external wall and with a central collecting electrode.

As a fast charged particle passes through a gas, both excited and ionized molecules are created and a neutral molecules ionisation release a positive ion and a free electron. This released ion pair is the basic constituent of the electrical signal formed in the ion chamber and the number of ion pairs created along the track of the radiation is the quantity of interest in this technique because, with knowledge of the average energy W required to produce an ion pair in a specific gas, is possible to estimate the deposited energy by the initial beam. The W quantity is a function of the species of gas present in the cavity, the type of radiation, and its energy.

Consequently, ionization chambers can be used for the measurement of the absorbed dose in arbitrary materials. For this, the Bragg-Gray principle, expressed by Equation 4.10, is applied. In this, S_m is the relative mass stopping power of the material to that of the gas and P the number of ion pairs per unit mass formed in the gas.

$$D_m = W\, S_m\, P \qquad \text{(Equation 4.10)}$$

All the correction parameters associated to the ionization chamber are very well known and that is why this technique is much recommended for beam calibration in radiotherapy. Also, they are quite used in diagnostic radiology for the determination of radiation doses because of the high accuracy and precision of the results.

This system is also preferred for the daily use in clinics because it displays the signal instantaneously and can be reused with no or very little change in the sensitivity. However, possible disadvantages are the need of connecting cables that might influence the treatment equipment and the fact that it requires a high voltage supply.

4.3.2. THERMO LUMINESCENT DOSIMETRY

The thermo luminescent dosimetry (TLD) system has been used by the IAEA's dosimetry laboratory to provide audits since 1969. As the name indicates, the system is based on the phenomenon of luminescence that occur in some materials when, upon the absorption of radiation, the absorbed energy is kept by electrons in metastable states and is then released in the form of ultraviolet, visible or infrared light when the dosimeter is submitted to heat. Luminescence can be classified as fluorescence when the light emission occurs within nanoseconds to milliseconds after the irradiation or as phosphorescence if the light emission takes seconds or even some minutes to occur.

The process of luminescence can be accelerated using an exciting agent like heat and, in this case, the phenomenon is called thermoluminescence. Two of the most commonly used dosimeter materials used in medical applications are based on lithium fluoride - LiF:Mg,Ti and LiF:Mg,Cu,P - because of their tissue equivalent properties.

More advantages of these dosimeters include the possibility to perform point dose measurements due to their small size and their linear response over a wide range of the doses used in radiotherapy. For some doses and materials, however, the dosimeter shows a supralinear behaviour and might even saturate. For example, the LiF:Mg,Ti dosimeter presents a supralinear behaviour for doses over 2 Gy.

During the readout, the signal is erased and, if not read carefully, some errors are quite easy to make, resulting in inaccurate results. From the TLD readout, correction factors like energy and fading corrections must be applied to obtain the correspondent absorbed dose.

TLD cannot be used for beam calibration but is very applied to perform dosimetry audits in radiotherapy.

4.3.3. ELECTRON PARAMAGNETIC RESONANCE DOSIMETRY

Electron Paramagnetic Resonance or EPR is well established spectroscopy method used to study matter with one or more unpaired electrons also known as free radicals. From the moment EPR spectroscopy started to be used for dosimetry purposes, it has been applied to several purposes: radiation dose reconstruction (retrospective dosimetry), identification of irradiated food, radiation therapy and also geological and archaeological dating.

EPR dosimetry in radiation therapy has progressed quite a lot in the past years and though many studies are still being made concerning it, using dosimeters with high sensitivity like the ones used in EPR dosimetry is thought to be one of the most advantageous methods in the field of radiation dosimetry regarding its accuracy.

4.3.3.1. Basic Principles

Depending on the number of electrons an atom has in its outermost shell (making it full of not) the atom is more or less stable and consequently more or less susceptible to create free radicals. Radicals are defined as molecular species that contain unpaired electrons in the atomic orbital [40] which are, in most cases, chemically reactive and try to interact with other molecules to achieve higher stability, behaving as oxidants or reductants. They can be formed by a spontaneous process or due to some environmental factors.

The creation of free radicals is a very important and biologically measurable effect of ionization radiation and is the basis of EPR spectrometry for dosimetry purposes. While most of the radicals formed react instantaneously and disappear, in some materials with crystalline structures where the diffusion is limited, the unpaired electrons can persist for long periods. The key issue in EPR is therefore to find these materials where substantial amounts of free radicals are created and stabilized after irradiation [31] so they can be easily evaluated and measured.

So far was found that some organic materials like amino acids, sugars, bone and tooth enamel present the needed crystalline structure and, when exposed to radiation, produce quite stable free radicals, being the ideal materials to be used in EPR spectroscopy. The basic principle in consideration to identify and quantify the number of the induced radicals is that the absorbed energy from ionising radiation is proportional to the number of unpaired electrons in the irradiated sample.

According to IAEA [8], EPR spectroscopy is defined as:

> "The measurement of resonant absorption of electromagnetic energy resulting from the transition of unpaired electrons between different energy levels, upon the application of radio frequency energy to a paramagnetic substance in the presence of a magnetic field"

The elementary concepts of this technique arise from the quantum mechanics. From that, is known that electrons are characterised by a magnetic moment and a spin quantum number $s = \frac{1}{2}$ with

magnetic components $m_s = +\frac{1}{2}$ (state of highest energy) and $m_s = -\frac{1}{2}$ (state of lowest energy) when a magnetic field is applied. Without any external magnetic influence, the magnetic moment will be randomly oriented but, when the electrons are exposed to an external magnetic field B_0, the spin can only be aligned parallel or antiparallel to the magnetic field operator and their orientation defines if the electrons are in the state of lowest or highest energy, respectively.

The splitting in the two energy states is called *Zeeman Effect* and is represented in Figure 4.1.

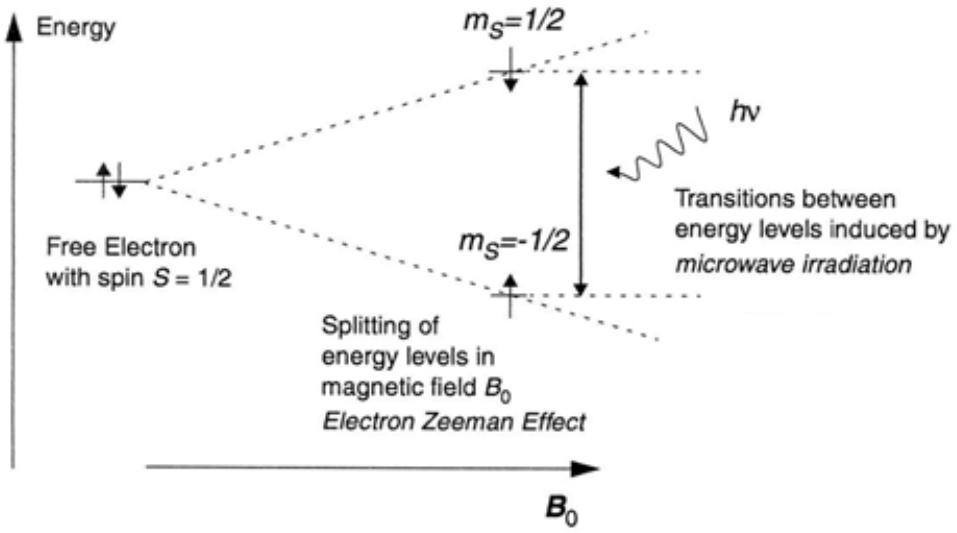

Figure 4.1 - Illustration of the Zeeman Effect in one free electron. The electron has spin ½ and under the influence of an external magnetic field B_0 it magnetic moment can be oriented either in parallel or anti-parallel to the magnetic field operator. Transitions between both states can be induced by microwave irradiation. Adapted from *[50]*.

The energy of the unpaired electron in each level [41] is given by the following Equation 4.11, where E_0 is the electron energy without any influence of the magnetic field, m_s is the magnetic moment of the electron, μ_B is the Bohr magneton[3], g is the g-factor[4] and B_0 the applied magnetic field.

$$E = E_0 + m_s \, \mu_B \, g \, B_0 \qquad \text{(Equation 4.11)}$$

Considering the symmetrical values that m_s can take, the difference of energy between the two states is also given by quantum mechanics and is expressed in Equation 4.12. This is considered the fundamental equation of EPR spectroscopy.

$$\Delta E = \mu_B \, g \, B_0 \qquad \text{(Equation 4.12)}$$

Any unpaired electron can move between the two energy levels by either absorbing or emitting a photon of energy $h\nu$ and, for that, the resonance condition in Equation 4.13 must be fulfilled.

$$\Delta E = h\nu \qquad \text{(Equation 4.13)}$$

So, an irradiation at a frequency ν that matches the difference ΔE will result in the absorption of energy and this frequency will also correspond to the resonance frequency of the electrons.

Since μ_B is a constant and the magnitude of B_0 can be measured, the way to determine g, the "fingerprint" of the molecule, is to determine the energy ΔE between the two spin levels.

[3] Physical constant and the natural unit of electronic magnetic moment. Its value is approximately 9.274 x 10^{-28}

[4] Proportionality constant that depends on the electronic configuration of the radical or ion

From equations 4.11 and 4.12 is easy to understand that without a magnetic field B_0 no energy difference can be measured and that the difference between the two levels of energy and the resonance frequency is linearly dependent on the magnetic field applied. This is represented on Figure 4.2 A.

In this way, it is possible to change the energy difference between the two spin states by varying the magnetic field strength and, taking this into account, there are two alternative ways to obtain a spectrum of the sample: either a constant magnetic field is applied and the frequency of the electromagnetic radiation is scanned in conventional spectroscopy or a static electromagnetic radiation is applied (constant frequency) with an oscillating magnetic field and the continuous wave is scanned, in the named continuous wave technique [42]. Due to the limitations of microwave electronics, the second method is the one preferred in dosimetry and consequently chosen in EPR spectrometry.

The absorption peak in the spectrum is obtained by means of EPR spectroscopy when Equation 4.12 is satisfied. When the magnetic field strength increases, the difference between the two spin states energies also increases until it equals the energy of the electromagnetic radiation and spin-flip transitions are induced, resulting in an absorption spectrum. This is represented in Figure 4.2 B.

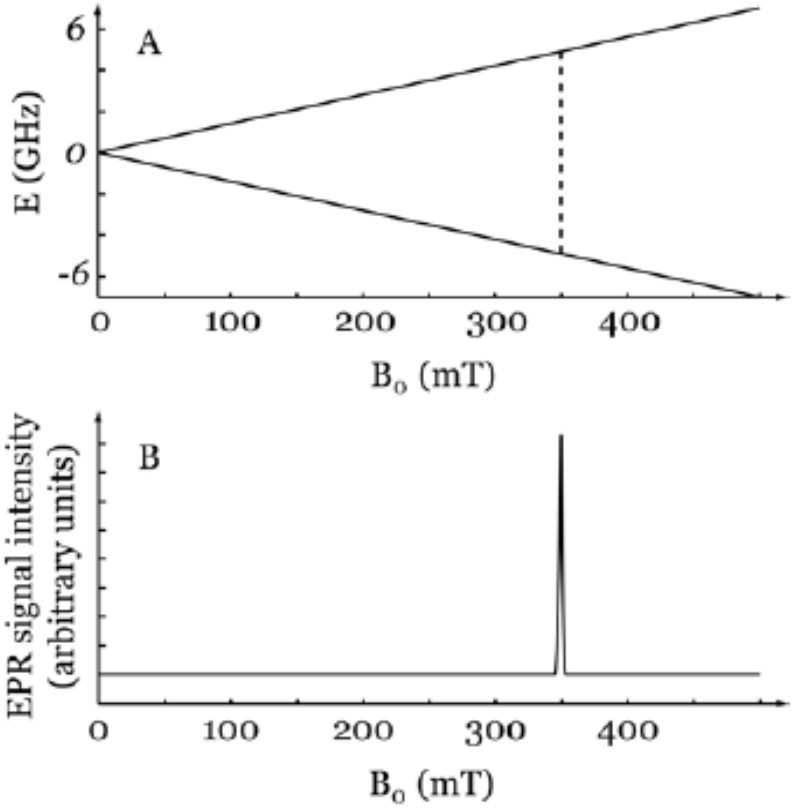

Figure 4.2 - A: Representation of the increase in the energy levels of an electron spin as the magnetic field applied increases. The dash line indicates the allowed EPR transition for 9.8 GHz photons. B: Simulated EPR absorption spectrum for the allowed transition. The spectrum line appears when the magnetic field tunes the energy difference of the two spin states, according to equation 4.12. *[46]*

The magnetic field at which the absorption peak occurs is named "field of resonance" and, as mentioned, is responsible for the resonance phenomenon of the electrons.

To obtain the signal, the microwave band of the equipment is defined previously or else the field of resonance could never be achieved. This band is associated with a frequency and a field of resonance and these parameters might vary according to the g factor. The typical microwave bands for a $g = 2$ signal are presented in Table 4.1 [43].

In this project the EPR spectrometer was used in the X-Band which is the most commonly used in applications of biodosimetry because it represents a good compromise between sensitivity and water content in the sample [44]. Since our interest is to use EPR for medical dosimetry purposes, this water criterion is very importance and should be considered.

Even though L and S bands could be used in samples with considerable water content, the sensitivity would be much lower than the X-Band. On the other hand, W and Q bands are more sensitive but are also quite affected by the water content and thus are not suitable for this application.

Table 4.1- Fields of resonance for the typical microwave bands available in EPR spectrometers. The most widely frequency used in EPR dosimetry is the X-Band.

Microwave Band	Frequency (GHz)	B_{res} (mT)
L	1.1	39
S	4.0	143
X	9.75	348
Q	34.0	1210
W	94.0	3350

4.3.3.2. EPR Spectroscopy

The EPR absorption spectrum is obtained by a specific equipment called EPR spectrometer. The equipment model used for the EPR readout in the test of this research is an Elexsys E500 EPR spectrometer and is schematically represented in Figure 4.3.

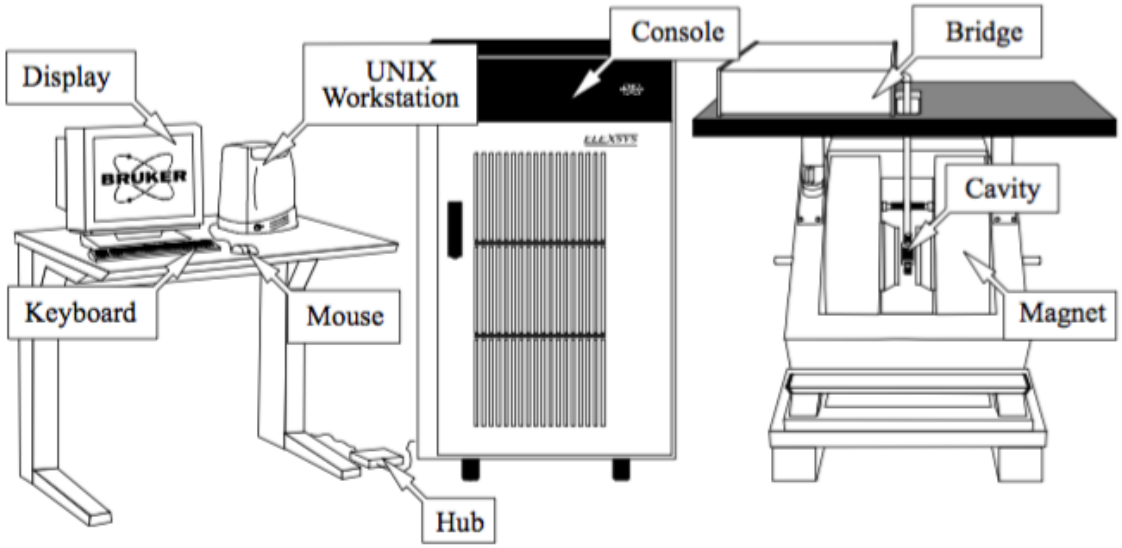

Figure 4.3 - Main components of an EPR Elexsys E 500 spectrometer. Is possible to distinguish the microwave bridge; the microwave cavity; the electromagnet that allows a controlled sweep of the magnetic field; the console that includes the signal channel and the computer where the output is displayed *[44]*.

This equipment includes not only the three components existent in any spectrometer - a source of electromagnetic radiation, a sample and a detector - but also some other components that should be taken into consideration due to their importance and will be briefly described.

The microwave generator and the detector are in a microwave module (or bridge). The dosimeter is placed in a sample tube positioned in a microwave cavity - or *EPR cavity* – which is the *heart* of the spectrometer, consisting in a metal box responsible for amplifying the weak signals from the sample. Cavities are characterized by their quality factor (Q) that is a measure of the efficiency with which the cavity stores the microwave energy: the bigger Q is, the bigger is the sensitivity of the spectrometer.

In the EPR cavity, the phenomenon of resonance occurs and the microwave energy upcoming from the generator is stored inside because, at the resonance frequency of the cavity, no microwaves are reflected. Consequently, a standing wave is created at the resonance frequency inside the cavity. A characteristic of standing electromagnetic waves is that their electric and magnetic field components are exactly out of phase so, when one is maximum, the other is minimum. The magnetic field is the one that drives the absorption in EPR so, if the sample is placed in the maximum magnetic field, the signal obtained will be the biggest and the sensitivity will also be higher.

The microwaves are coupled in the cavity via a hole called iris, whose size can be adjusted by an iris screw. The size of the iris determines the amount of microwaves that will be reflected back from the cavity and how much will enter the cavity. This is automatically done by the iris by cautiously matching or transforming the impedances of the cavity and the waveguide (that leads the microwaves to the cavity).

When the sample absorbs microwave energy, the Q factor is lowered due to the energy losses and, at the same time, the impedance of the cavity is altered leading to changes in the coupling condition. Therefore, the cavity is no longer coupled and the microwaves are reflected back to the bridge, originating the EPR signal.

The fixation of the sample tube in the EPR cavity must be very robust and precise to avoid disturbing the magnetic field and make possible the reproducibility of the measurements.

The signal channel is the unit that fits the spectrometer console and contains all the electronics for a phase sensitive detection. It provides amplification, processing and recording of the microwave absorption in the sample while the magnetic field scans the resonance condition.

The magnetic field controller also has a great importance because it is responsible for superimposing a rapidly varying small magnet field and, in this way, allowing a controlled and precise sweep of the magnetic field for the EPR measurements.

The magnetic field regulation occurs via a Hall probe placed in the gap of the magnet. This probe produces a voltage dependent on the magnetic field that is perpendicular to the probe and the magnetic field is regulated by comparing the voltage from the Hall probe with the reference voltage given by the other part of the controller. When these voltages do not match, a correction voltage is sent to the magnet power supply that changes the amount of current going through the magnets and, thus, the magnetic field. When the difference is null, the magnetic field is considered stable and is locked. In this way, the microwaves reflected from the cavity are amplitude modulated at the same frequency and only these amplitude-modulated signals are detected and contribute to the EPR signal, decreasing the signal-to-noise ration (SNR).

The choice of the modulation amplitude and frequency by the user have, therefore, to be done wisely so that the best signal is obtained. Usually, for measurements in the X-band frequency, the modulation frequency is set to 100 kHz.

Within the width of the modulation amplitude, the absorption signal is approximately linear and the slope of the signal determines the presented wave amplitude, being proportional to each other.

So, as shown in Figure 4.4, the absorption signal is transformed into a sinusoidal wave that is the first derivative of the absorption spectra. The signal intensity is the peak-to-peak-height of the signal.

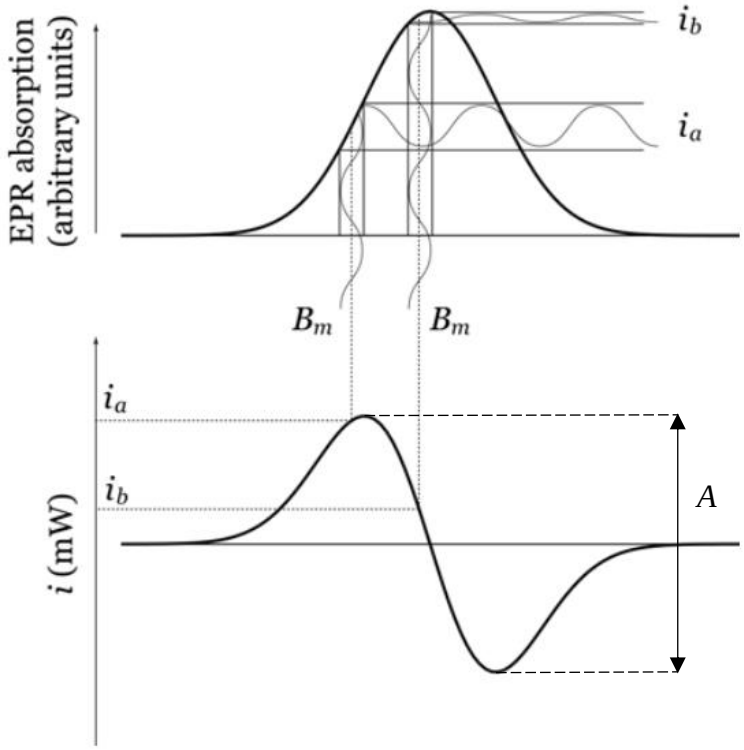

Figure 4.4 - Illustration of the EPR absorption line and the respective first derivative, as the EPR signal is presented in the EPR spectroscopy technique. The absorption signal is measured using a modulation amplitude B_m and a constant modulation frequency ν and the amplitude i is dependent on the slope in the absorption spectrum and oscillates with the modulation frequency. The peak-to-peak height A is interpreted as the signal intensity. *Figure adapted from [46]*

Lastly, the readout is displayed on the computer screen that is connected to the console. It is in this computer that, in the EPR software, all the microwave and signal channel parameters are adjusted.

In the obtained sinusoidal wave, the peak-to-peak amplitude (parameter A in Figure 4.4) is proportional to the number of $\frac{1}{2}$ spins which is, by its turn, related to the radiation-induced radicals or absorbed dose: the main interest of dosimetry.

The readout technique is non-destructive to the signal and the sample can and must be read several times to improve measurement precision and reduce possible instabilities in the spectrometer that might influence the magnetic field. According with previous studies [45] three readouts of each dosimeter is enough to decrease the relative standard uncertainty of the measurements to 0.60 % and therefore obtain more precise values.

4.3.3.3. Advantages of lithium formate EPR Spectroscopy

The purpose of using lithium formate EPR in radiation therapy arises from the many advantages that this dosimetry technique might over some other dosimetric systems, either active methods like ionisation chambers and passive methods like thermoluminescence dosimetry systems, for example.

The first important characteristic of EPR comes from the fact that it is a passive method and is also an advantage of TLD. Although it does not present the result instantaneously and require some

calibrations and signal analysis, the response of these systems is not dependent on the direction of the beam because there is no wiring that might disturb the radiation field [19]. Passive dosimetry methods can therefore be one option for dose verifications in IMRT treatments where the existence of cables can complicate the dose measurement in some cases.

In comparison to other passive methods, EPR is a more advantageous method for its linear dose response over a larger dose range so it can be suitable for dose monitoring in various measurement situations, either in phantom verifications or in in-vivo measurements. Another benefit is that the dosimeter signal is not affected by the dosimeter readout process, unlike the TLD systems, so it can be measured multiple times without having erased the signal. This is very important because, as referred before, repeating the measurements several times will reduce considerably the uncertainty associated to the measurement.

Nonetheless, apart from the properties of the technique itself, the advantages are even more enhanced with the possibility to choose a tissue equivalent dosimeter material. This is, if a high sensitive dosimeter material like polycrystalline lithium formate monohydrate is used to manufacture the dosimeters, a much more precise measurement of the absorbed doses is possible as a result of the similar behaviour of radiation regarding the scattering and absorption of ionising radiation in the dosimeter material and in body tissues.

In comparison with alanine, the reference material for EPR dosimeters, lithium formate has a relatively higher sensitivity and, even though there are some more sensitive materials (ammonium formate or potassium dithionate), lithium formate is considered the best option among other materials precisely because of the tissue equivalent and hydroscopic characteristics [46]. Ammonium formate, for example, is a good alternative regarding the tissue equivalence characteristics but is highly hydroscopic which makes it not suitable for the purpose.

Also, the availability of lithium formate in the market is a relevant factor because it allows an easy, fast and cheap way to produce dosimeters.

All the above characteristics make EPR dosimetry a quite robust method in the measurement of almost every radiation range and a good alternative to the other methods.

The EPR dosimetry disadvantages are related with the readout equipment which is quite expensive and requires some parameters and technical knowledge. The readout process, if three to four measurements are to be made, is also considerably time consuming (around 4 minutes for each reading). Additionally, the EPR dosimeter is quite sensitive to some factors that might lead to erroneous measurements like water, temperature – an important factor during the irradiation process - and humidity that should be controlled during the storage of the dosimeters.

Chapter 5

MATERIALS AND METHODS

The lithium formate EPR dosimetry has been developed, tested and optimized for photon beams and this technique is becoming a realistic option for clinical dosimetry applications mostly because of its great accuracy.

For heavy particle beams, the variation of the LET along their track suggest a non-homogeneous dose deposition in the target and that non-homogeneity might result in some differences in the performance of the dosimetry system, which should be assessed before it is considered a viable option for dose verifications.

To well characterize the lithium formate dosimetry system for proton beams, the further described methodology was followed.

The project is divided in several steps performed both in the city of Linköping (Sweden) as in Uppsala (Sweden): the lithium formate dosimeters manufacture and acceptance through a homogeneity check were made in Linköping University as well as all the EPR readouts and respective analysis and all the proton irradiations necessary to the characterization of the lithium formate dosimetry system were made in the first and only specialized centre for proton therapy in Scandinavia[5]: the SkandionKlinik, in Uppsala.

5.1. Batch Production and Acceptance

5.1.1. Dosimeter Production

The dosimeters are hand-made and manufactured in batches of ten to thirty dosimeters, containing the same mixture of lithium formate monohydrate and paraffin that is used as a binder.

For each experiment, a new batch of dosimeters is produced.

[5] Region that comprises Denmark, Norway and Sweden

The procedure begins by sieving an amount of polycrystalline lithium formate monohydrate (98 %) (HCO_2LiH_2O) to a grain size between 180 microns and 500 microns using an Endecotts MINOR sieve shaker. Then, depending on the mass of the lithium formate sieved, paraffin is added to make the tablets stable and non-fragile. The amount of solid paraffin to add is calculated so that paraffin constitutes 10 % of the total weight of the powder.

To melt the paraffin and mix it well with the lithium powder, the mixture is placed in a beaker and heated for 15 minutes in an oven with 88˚C. This temperature is chosen so that it is higher than the melting point of paraffin and lower than the melting point of the lithium formate, which are 60 ˚C and 94 ˚C, respectively. After the heating, the content is removed from the oven and is carefully mixed until it returns to room temperature. The heating and mixing process is repeated three times to guarantee that the two materials are well mixed, in the most homogeneous way.

Then, the mixture is kept for about one hour at the room temperature to solidify the paraffin before the mixture is ready for the dosimeters production in the tablet pressing procedure.

An amount of 102.0 mg to 103.0 mg of powder is weighted, placed on the cup of the table-top pellet-press shown in Figure 5.1 and by pushing the punch down during some seconds, the powder is pressed and forms a compact cylindrical dosimeter with diameter 4.5 mm and height 4.9 mm.

Figure 5.1 - Table-top Pellet-press used for producing the dosimeters. The equipment defines the dosimeters cylindrical shape.

The final weight is verified and if it is in the interval 100.0 ± 1.5 mg the dosimeter is labelled at its bottoms and kept in a dark glass jar with cotton inside to protect the dosimeter from any possible physical damages and UV light radiation. The dosimeters are named according to a system where each receives a letter and a certain number of dots (one to five), as shown in Figure 5.2, so each receives an identity like aI, aII,aIII, bI, etc.

The process is repeated until the number of dosimeters wanted is obtained.

To reduce even more any possible external influence due to environmental changes, all the jars containing the tablets are stored in a desiccator with a stable and controlled relative humidity of 35 %. In this way, all dosimeters from the same batch are stored in identical conditions and treated equally.

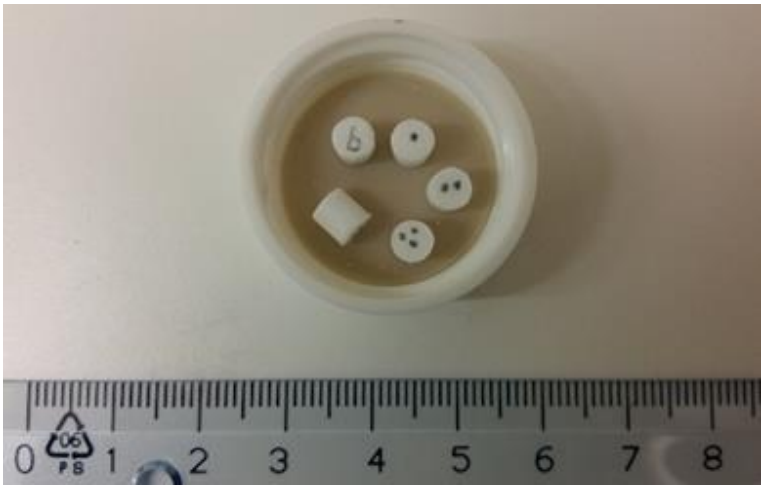

Figure 5.2 – Five dosimeters labelled according to the system chosen. In one bottoms the letter representing the group is written and in the other bottom the dots are drawn. One of the dosimeters from the group is shown by side to give a realistic perception of the dimensions of the tablets.

5.1.2. HOMOGENEITY TEST

After the production of the dosimeters, is important to verify that the response of every dosimeter is similar when they go through the same conditions and absorb the same dose and this is verified if no properties have been altered during the production process or storage conditions due to, for example, contamination or humidity. To guarantee that no dosimeter characteristics were altered and that they all maintain similar properties, the homogeneity test is performed.

To do so, the dosimeters are firstly positioned in a PMMA phantom represented in Figure 5.3 with twenty holes drilled in a circle and equidistant from the centre in order to guarantee that all dosimeters are irradiated with the same energy.

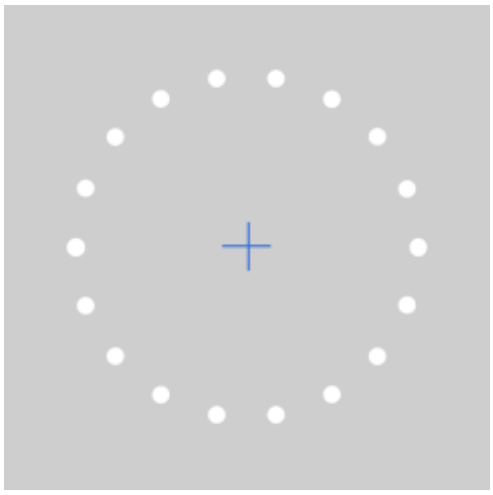

Figure 5.3 - Schematic representation of the PMMA phantom used for in Homogeneity Test. The phantom of dimensions 15*15*0.5 cm^3 has twenty holes drilled in circle with a size that allows the insertion of the dosimeters. The + sign is positioned in the irradiation field centre.

The PMMA phantom is then centred in a 10 x 10 cm^2 square irradiation field and slabs of PMMA are added on the top of the phantom so that the dosimeters are placed at a depth of 8.5 cm equivalent to 10 cm water using density scaling. The source-surface distance (SSD) is adjusted to be 100 cm. Finally, a 3 Gy irradiation is performed using a 6 MV photon beam by a linear accelerator.

If the batch has more than twenty dosimeters, the procedure must be repeated until all of them are irradiated and if there are not enough dosimeters to fill all the holes, dummies of the lithium formate dosimeters must be used to fill them.

After the irradiation, the signal of each dosimeter is read using a spectrometer BRUKER EleXsys E500 with the procedure described in section 5.2 and the results are analysed using the software Matlab Student R2016a and Microsoft Excel 2016.

To accept a batch as homogeneous, two criteria must be fulfilled:

- No individual EPR signal must deviate more than 2 % from the average EPR signal of the whole batch;
- The relative standard deviation (RSD) of the signals of all dosimeters must lower than 1 %.

The RSD is calculated with Equation 5.1, where s is the standard deviation of all the signals obtained and $\bar{x}$ the mean signal of every dosimeters signal.

$$RSD\ (\%) = \frac{s}{\bar{x}} \times 100 \qquad \text{(Equation 5.1)}$$

However, if the RSD is bigger than 1 % the batch can still be accepted and used if corrections to the signals are made. For this reason, an individual calibration factor (ICF) is also calculated for each dosimeter n using Equation 5.2. This factor is the quotient between each signal EPR_n read in the spectrometer and the average $\overline{EPR}$ of all dosimeters signals.

$$ICF_n = \frac{EPR_n}{\overline{EPR}} \qquad \text{(Equation 5.2)}$$

The ICF is used as a correction factor that is applied to the obtained signal.

The individual corrected signal of dosimeter n $EPR_{c,n}$ is therefore obtained by the quotient in Equation 5.3 where EPR_n is the signal read in the spectrometer of dosimeter n and ICF_n is the individual calibration factor calculated for the same dosimeter.

$$EPR_{c,n} = \frac{EPR_n}{ICF_n} \qquad \text{(Equation 5.3)}$$

5.2. EPR READOUTS

EPR spectra are recorded at room temperature using a BRUKER E500 EleXsys EPR spectrometer operating at the X-band and equipped with a standard ER4102ST resonator cavity.

Each dosimeter, once at a time, is positioned in the bottom of a glass tube with 5mm inner diameter and flat bottom. One of the most important factors to be able to reproduce the measurements and compare the several results obtained is the guarantee that all dosimeters are placed in the exact same position in the tube for every measurement.

Additionally, the glass tube is held by a pedestal essential to ensure that the tube is placed in the exact same position for each measurement.

The spectrometer settings are defined according to Table ***5.1.***

Table 5.1 – Spectrometer settings for EPR measurements. All the settings were defined according to previous experiments to obtain an optimal signal. The Center Field value is the one parameter that is adjusted to guarantee that the peak to peak is in the obtained spectrum range.

Microwave Power	20 mW
Modulation Frequency	100 kHz
Modulation Amplitude	1.2 mT
Field Width	3 mT
Conversion Time	168 s
Time Constant	328 s
Receiver Gain	60 dB
Center Field	~ 347 mT

Each dosimeter is ideally read out 4 times in a rotating schedule: all dosimeters from the batch are read one time in a sequence and then the readout process is repeated. In this way, each readout is spread out during the day and any possible errors due to the variation of the spectrometers sensitivity are reduced. The choice of performing four readings of the dosimeters is justified by the previous conclusions of related experiments [45].

The signal intensity is obtained by calculating the peak-to-peak height in the first derivative of the absorption spectrum given by the software and similar to the one represented in Figure 4.4. Since the signal is read more than once over the day, the real signal associated to each tablet is defined as the mean value of all the readings made of that specific dosimeter.

5.3. LITHIUM FORMATE DOSIMETRY SYSTEM: CHARACTERIZATION

All the irradiations needed for the tests that are now described were performed in Skadionkliniken in Uppsala using a proton beam with associated energy of 150 MeV.

To irradiate the dosimeters, they are placed in a five-hole PMMA phantom, represented in Figure 5.4. In this phantom with 0.5 cm height, four dosimeters are placed in the outside holes equidistant from the centre and a dummy is placed in the centre hole so that all holes are filled.

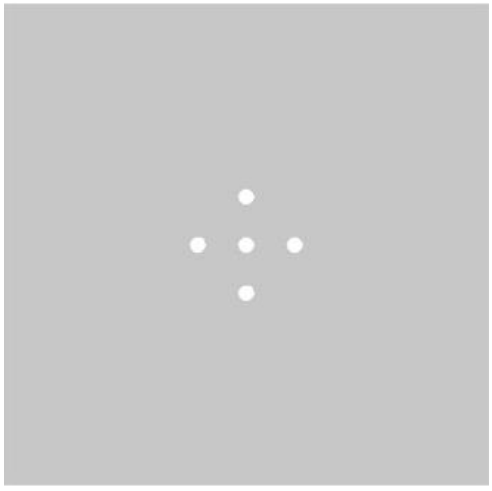

Figure 5.4 - Schematic representation of the PMMA phantom used for the proton beam irradiations. The phantom of dimensions 18*18*0.5 cm^3 includes five cylindrical holes: in the middle hole a dummy is inserted and the dosimeters are put in the four surrounding holes

The PMMA phantom is placed over a 5.0 cm slab of solid water and the dosimeters and one dosimeter dummy are placed in the respective position (Figure 5.5 A). Then, the phantom is centred with the 10*10 cm^2 irradiation field and additional slabs of solid water were added to reach 2.7 cm of solid water over the PMMA phantom (Figure 5.5 B).

A depth of 2.7 cm in solid water corresponds to a 2.76 cm depth in water and, accounting the dosimeter height of 0.5 cm, the centre of the PMMA phantom and, thus, the centre of the dosimeters height were placed at an approximate depth of 3 cm. The 3 cm value is the reference depth for the reference dosimetry at this energy.

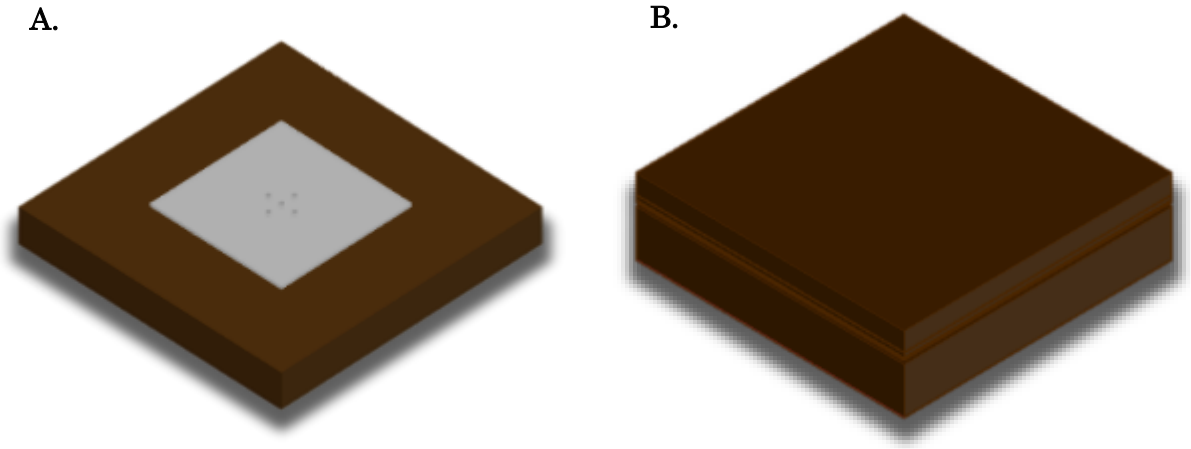

Figure 5.5 – Schematic representation of the experiments set-up for the proton beam irradiations. A: the PMMA phantom (in grey) where the dosimeters and the dummy inserted is placed over a 5 cm slab of solid water (in brown) and centered with the center of the irradiation field. B: Additional 2.7 cm of solid water are added over the phantom to achieve the conventional depth used for the reference dosimetry

All the necessary irradiations needed for both linearity test and fading test described next were performed using this set-up.

5.3.1. LINEARITY TEST

The first test is regarding the dose dependence of the dosimetry system: as mentioned the response must be independent of the dosimetry quantity measured.

A homogeneous batch of twenty-four dosimeters is produced, tested regarding its homogeneity and divided in six sub-groups of four dosimeters each. From the homogeneity analysis, the ICF values were calculated and saved to be used if homogeneity corrections were needed.

All the dosimeters were transported to SkandionKliniken inside the UV light protected and air-tight glass bottles and are only removed from the bottles to carry out the irradiations that were all made in the same day.

Once at a time, each of the dosimeter group is placed in the PMMA phantom in the treatment gantry and irradiated with a radiation dose between 0 Gy and 9 Gy. The group that received no dose was also transported to Skandion and put in the treatment gantry so that its dosimeters would experience the same circumstances as the other dosimeters.

An ionization-chamber dosimetry control is made before the irradiations to check the reference doses of the proton system. From the assumption that the $k_{Q, Q0}$ [6] is the same for water and solid water, the measured reference dose of the proton system used is 0.68 Gy per field.

As the irradiations were not previously planned – there was no defined dose plan - and to make the setup easier, the irradiated doses to each group are multiples of the reference dose and the number of fields applied to each group of dosimeters varies from 0 to 13 as Table ***5.2*** shows.

Table 5.2 – Absorbed doses by each sub-group of dosimeters in the Linearity Test. The doses given were multiples of the reference dose of the system (0.68 Gy per field) and the multiples were chosen so that the doses would be as equally spaced as possible. Group 6 was also carried to the clinic but its dosimeters received no dose.

Group	Reference Dose per field (Gy)	Number of fields applied	Dose (Gy)
a	0.68	2	1.36
b	0.68	4	2.72
c	0.68	7	4.76
d	0.68	10	6.80
e	0.68	13	8.84
f	0.68	0	0.00

After the irradiations, the dosimeters are carried back to Linköping and the dosimeter signals are read following the procedure described at section 5.2.

[6] Refers to the chamber-specific quality factor that corrects the chamber response for differences between the reference beam quality Q_0 (^{60}Co) and the quality Q of the given beam

Due to practical issues regarding the distance between Uppsala and Linköping and the time needed to perform all the signal measurements, these are not done in the same day as the irradiations but in one of the days following the irradiations.

Once all the signals are read, Matlab Student R2016a is used to extract the data from the obtained signals and those signals are analysed both in Matlab and R.

From the signals a calibration curve is determined to characterize the response of the system to the different absorbed doses by each group and conclusions are taken regarding the linearity (or non-linearity) of the system.

5.3.2. BLIND TEST

To support the linearity test, a blind test was performed to verify how precisely the absorbed dose could be predicted from the dosimeter EPR signals once the linear behaviour of the system, expressed by the calibration curve, is determined.

For this end, a batch of twelve dosimeters was manually produced, tested regarding its homogeneity and divided in three groups of four dosimeters each. Each group was placed inside UV light protected and air-tight glass bottles and were only removed from the bottles to perform the irradiations, in SkandionKliniken, and the EPR readouts, in Linköping University.

The dosimeters were taken to SkandionKliniken and, there, one of the groups was not irradiated with the clinical proton beam (the zero dose point in the calibration curve), one group was irradiated with 7.90 Gy (the second dose point needed to determine the calibration curve) and the third group was irradiated with an intermediate dose, defined by the medical physicist and unknown to the experimentalist.

The doses absorbed by each group from the proton beam are expressed in Table ***5.3***.

Table 5.3 – Absorbed doses by each sub-group of dosimeters in the Blind Test. Two of the groups were irradiated with known doses and the dosimeter signals will be used to estimate the calibration dose curve. The other group received a dose unknown that will be estimated from the dosimeter signals.

Group	Dose (Gy)
a	0.00
b	?
c	7.90

After all the irradiations needed, the dosimeters are carried back to Linköping University and the EPR signals are read in the EPR spectrometer.

All signal information is analysed using both Matlab Student R2016a and R and, with the EPR signals of the dosimeters whose absorbed dose is known, the calibration curve that characterizes the system linearity is estimated and a prediction is made regarding the unknown dose.

5.3.3. FADING TEST

Another important characterization of the dosimetry system concerns the signal fading over time. To do so, a new batch of dosimeters is produced, tested for homogeneity and 24 dosimeters are selected. From these, six groups of four dosimeters each are formed taking into account the ICF values of the dosimeters and each group is placed in a different glass bottle.

Following the methodology of previous tests regarding the EPR system, all groups of dosimeters were carried to SkandionKliniken in the same day and stored there. During a period of one month, each week one of the groups is randomly chosen and is irradiated with approximately 8.84 Gy under the same conditions. After a group irradiation the dosimeters are stored in their respective UV-protected glass bottle and must not undergo any other irradiation or be used again until the EPR readouts.

Since the irradiations are done in different weeks and the proton beam characteristics vary slightly from week to week, the ionization chamber measurements registered a slight variation between the doses absorbed by the different groups. These doses and the dates of when the irradiations happened are explicit in Table ***5.4***.

Table 5.4 - Register of the absorbed doses by each of the groups irradiated. Once a week during one month each one of the groups was irradiated with approximately the same dose. The last group irradiated (group 6) was used as the reference group to normalize all the other signals.

Group	Irradiation Date (yyyy/mm/dd)	Dose (Gy)
a	2017/ 02/ 06	8.82
b	2017/ 02/ 13	8.76
c	2017/ 02/ 20	8.87
d	2017/ 02/ 27	8.82
e	2017/ 03/ 06	8.85
f	2017/ 03/ 07	8.83

Additional to the five groups irradiated with one week apart, there was also a sixth group irradiated one day after group *e* irradiation. This is made so that group *f* can be used as a reference group (to which no fading is considered) and its EPR signal is used to normalize all the other dosimeter group EPR signals.

After all irradiations, to analyse the fading associated to each group of dosimeters, all dosimeters are carried back to Linköping in the same day and read out two days after in the EPR spectrometer (due to the impossibility of doing it in the day after). The choice of reading all signals in the same day is justified with the results of previous similar tests where irradiating various groups in different weeks and all dosimeter readouts in the same day was a very successful attempt of minimizing the uncertainties resulting from the variations in spectrometer performance and consequent instabilities.

With the obtained signals, Matlab Student R2016a is again used to extract the information needed, results are analysed both in Matlab as in R and conclusions regarding the stability and signal fading of the dosimetry system are taken.

Chapter 6

RESULTS AND DISCUSSION

Following the methodology described in the previous section, the results of each test made in order to characterize the lithium formate EPR dosimetry system are now presented.

Each test analysis includes three sub-sections.

Firstly, the homogeneity test results for the respective batch used is analysed and the decisions regarding the acceptance of the dosimeters and the need (or no need) to use the ICF values are presented.

Secondly, the main results of the test are presented and a statistical analysis is made to include the errors associated to the measurements.

In the last section, the results are discussed and compared with previous findings related to the EPR dosimetry subject.

6.1. Linearity Test

6.1.1. Batch Homogeneity Analysis

A batch of 24 dosimeters was produced and, before its use, the homogeneity was verified.

For the homogeneity test, the dosimeters EPR signals were only read three times instead of the four times planned. This happened because no time was left to perform the fourth reading round due to some instabilities of the spectrometer over the day: many readouts had to be repeated when inconclusive results were obtained and also the settings needed to be readjusted sometimes.

The results from the homogeneity test are shown in Figure 6.1 where the black circles represent each dosimeter EPR signal obtained as the average of the three measurements made. Together with the representation of the individual dosimeter signal, error bars correspondent to the biggest deviation of the readouts made to the average signal of each dosimeter were added.

This analysis is made to guarantee that all the dosimeters readings were coherent i.e. that despite the possible instabilities of the spectrometer the measured signals from the same dosimeter are similar and do not vary significantly.

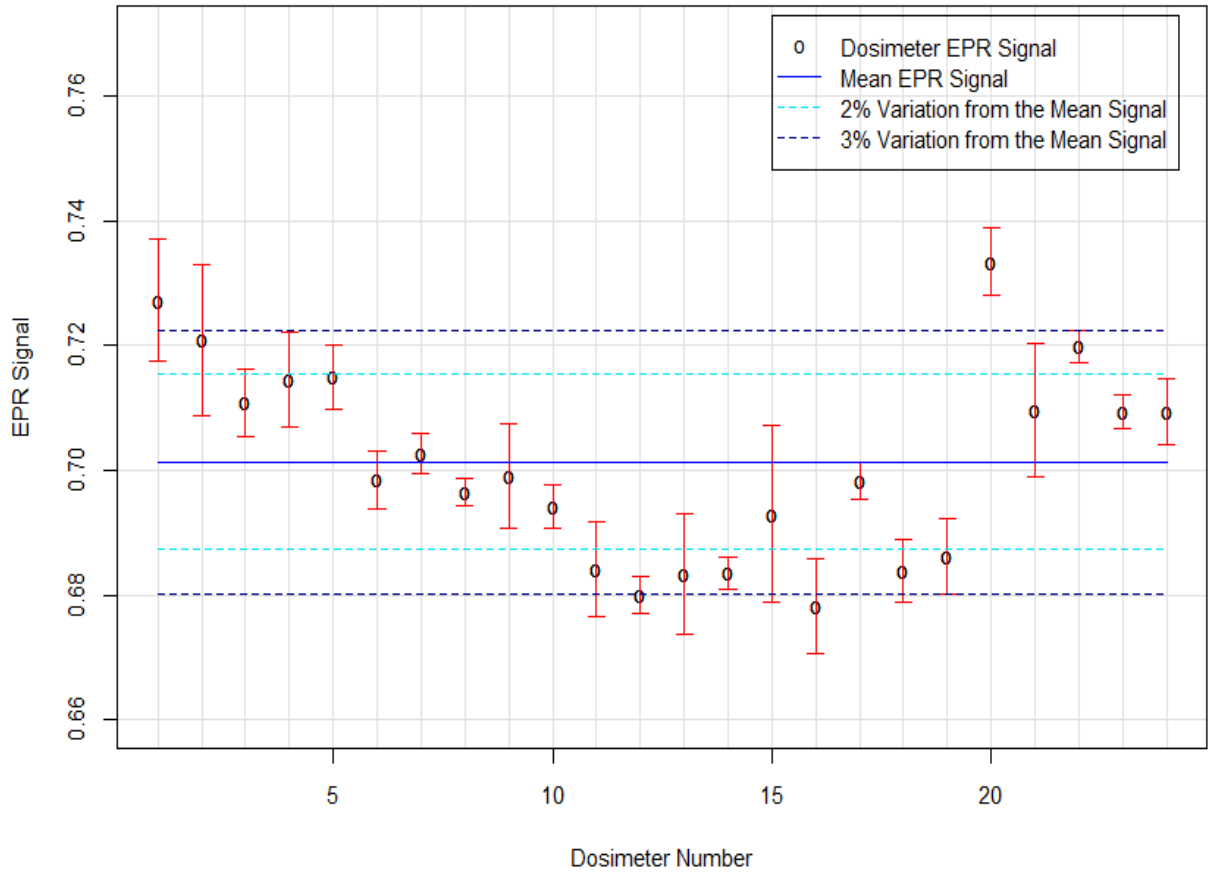

Figure 6.1 - Homogeneity analysis of the batch of dosimeters used in the Linearity Test. The circles represent the average EPR signal obtained from the three measurements done along the day. The red error bars represent the biggest deviation from the mean value of the three measurements performed to each dosimeter. The light blue and dark blue dashed lines are indicative of the 2 % variation and 3 % variation, respectively, from the whole batch EPR signal mean value that is one of the criteria to conclude about the homogeneity.

Taking that into, by reading the signal three times the average deviation is 0.53 % which is a very satisfactory result. The highest deviation associated to the individual signals was obtained for dosimeter number 15 in Figure 6.1 and took the value of 1.42 %. Besides this one, only other two dosimeters had readouts with a variation higher than 1 %: dosimeters number 2 and 21. Consequently, the results indicate that the small variations of the signals correspondent to the same dosimeter are more likely to be related to sporadic instabilities of the spectrometer that were not noticeable and could not be corrected and not related to the specific characteristics of the dosimeters. Therefore, all dosimeters are considered valid to be used.

Subsequently, the batch homogeneity was verified.

In an ideally homogeneous batch, no individual dosimeter signal should deviate more than 2 % from the mean signal of the whole batch. With knowledge of the average EPR signal, presented in Table ***6.1*** the 2 % limit would imply that every dosimeter signal would be in the interval [0.687; 0.715] delimited by the light blue dash lines in Figure 6.1. From this figure and from the signal values obtained is easy to verify that this is only verified to 13 of the 24 dosimeters produced (nearly 54 % of the batch). However, it is also easy to visualize that the signals are not very spread and for that reason an analysis considering a variation of 3 % of the mean signal was also made and is shown in Figure 6.1 by the dark blue dashed lines. The 3 % variation accepts dosimeters which signal is in the interval [0.680; 0.722] and in this case 20 in the 24 dosimeters produced verify the condition which corresponds to about 83 % of the whole batch but still does not include the whole batch.

From this is possible to state that the criteria regarding the variation of the individual signals is not fulfilled and the batch is not considered homogeneous. Yet, the statistical measures needed to take conclusions about the second homogeneity criteria were calculated and are presented in Table ***6.1***.

Table 6.1 - Overall analysis of the batch to be used in the Linearity Test. The average EPR signal calculated considering all dosimeters is presented as well as the standard deviation associated to all signals. Considering the values of these two quantities, the relative standard deviation is also shown.

Average Signal	0.701
Standard Deviation (%)	1.6
Relative Standard Deviation (%)	2.2

The relative standard deviation that represents the deviation of the individual signals around the mean signal and takes the values of 2.2 %, a value much higher than the 1 % limit defined as the second homogeneity criteria. This confirms that the differences of the dosimeters EPR signals are rather significant and the signal variation is most likely attributed to the differences in the individual dosimeters composition regarding the percentage of lithium formate and paraffin. Despite all the mixing process during the production of the initial mixture, there is no way to guarantee that a perfectly homogeneous mixture is achieved and that all portions used to manufacture each dosimeter have the exact composition. Consequently, even the smallest differences in the quantity of lithium formate in the dosimeters lead to slightly different EPR signals.

After this analysis, since none of the two criteria for homogeneity is verified, the batch is not considered homogeneous. Despite this, all dosimeters are considered valid to be used and, to contour the non-homogeneity, the individual calibration factors are calculated to each dosimeter using Equation 5.2 and must be used for further correction of the EPR signals.

6.1.2. LINEARITY TEST ANALYSIS

The batch of dosimeters was divided in six groups of four dosimeters and the linearity test was then performed. After the irradiations needed each dosimeter signal was obtained as the average signal of the four readouts done in the spectrometer over the day.

Before the analysis it is important to realise, firstly, that the absorbed doses mentioned in this section correspond only to the dose absorbed during the proton beam irradiation even though a dose of 3 Gy had already been absorbed by all of them during the homogeneity test. In this way, it is expected that no dosimeter has a null EPR signal. Secondly, as decided before, all the EPR signal obtained in the spectrometer after the proton irradiations were corrected with the correspondent individual calibration factor and the signal values here presented already account that correction.

A first analysis to the EPR signals of each group of dosimeters is made and presented in Table ***6.2***. For each group of dosimeters, the values regarding the absorbed dose, the mean EPR signal, the standard deviation and the relative standard deviation were calculated.

Table 6.2 - Summary of the EPR signals measured to each of the irradiated groups in the linearity test. The average signal of the four dosimeters of each group is presented as well as the associated standard deviation. Also, for a better comparison between the groups, the relative standard deviation of each group was also calculated.

Group	Absorbed Dose (Gy)	Average EPR signal	Signal Standard Deviation (%)	Signal Relative Standard Deviation (%)
f	0.00	0.644	0.4	0.6
a	1.36	0.915	0.3	0.3
b	2.72	1.206	0.8	0.7
c	4.76	1.623	0.5	0.3
d	6.80	2.027	1.9	0.9
e	8.84	2.427	7.2	3.0

The first conclusion is that, as expected, the average EPR signal increases as the absorbed dose by the dosimeters also increases. Concerning the standard deviation values, no linear behaviour is visible and this quantity varies quite randomly between the several groups so no correlation with the absorbed dose increase appears to exist.

In theory, every dosimeter absorbing the same dose should present the same EPR signal and, consequently, the mean EPR value of the group must be a good representative of each dosimeter signal of that same group. To analyse this, the relative standard deviation is more significant since it indicates how much the dosimeters signals vary around the respective group mean signal. Evaluating this quantity, five of the six groups present a relative standard deviation below 1 %, which is a very positive result and means that the dispersion of the individual signals of each group around the respective mean signal is minimal. Only group *e* has a relative standard deviation of 3 % that is considerably higher than the other but this bigger values does not seem to be related with the higher absorbed dose since no linear behaviour is observed between the two variables: the absorbed dose and the groups relative standard deviation.

Overall, as expected, no big dispersion is found among the groups dosimeter signals and is possible to state that the precision of the signal values within the same group is very satisfactory.

With the precision of each group evaluated, the necessary analysis to obtain information regarding the overall behaviour of the dosimetry system was made with the aim of verifying if the system dose response is dependent on the absorbed dose or, in other words, to verify if the relation between the absorbed dose and the EPR signal is in fact linear or not.

For an overview of the system and dosimeters response all signals are represented in function of the absorbed dose in Figure 6.2. Additionally, the regression that best fit the data is also represented by the dark full line.

The relation between both variables is clear as the detected EPR signals increase in a very linear way with the increase of the absorbed dose by the dosimeters. These findings are supported by the fact that regression model that best fit the data is, in fact, a linear model. The equation of this regression is expressed in Equation 6.1where S is the EPR signal and D the absorbed dose by the dosimeters. Each parameter has an associated uncertainty due to the signal measurement uncertainties.

$$S = (0.202 \pm 0.001) \times D) + (0.648 \pm 0.003) \qquad \text{(Equation 6.1)}$$

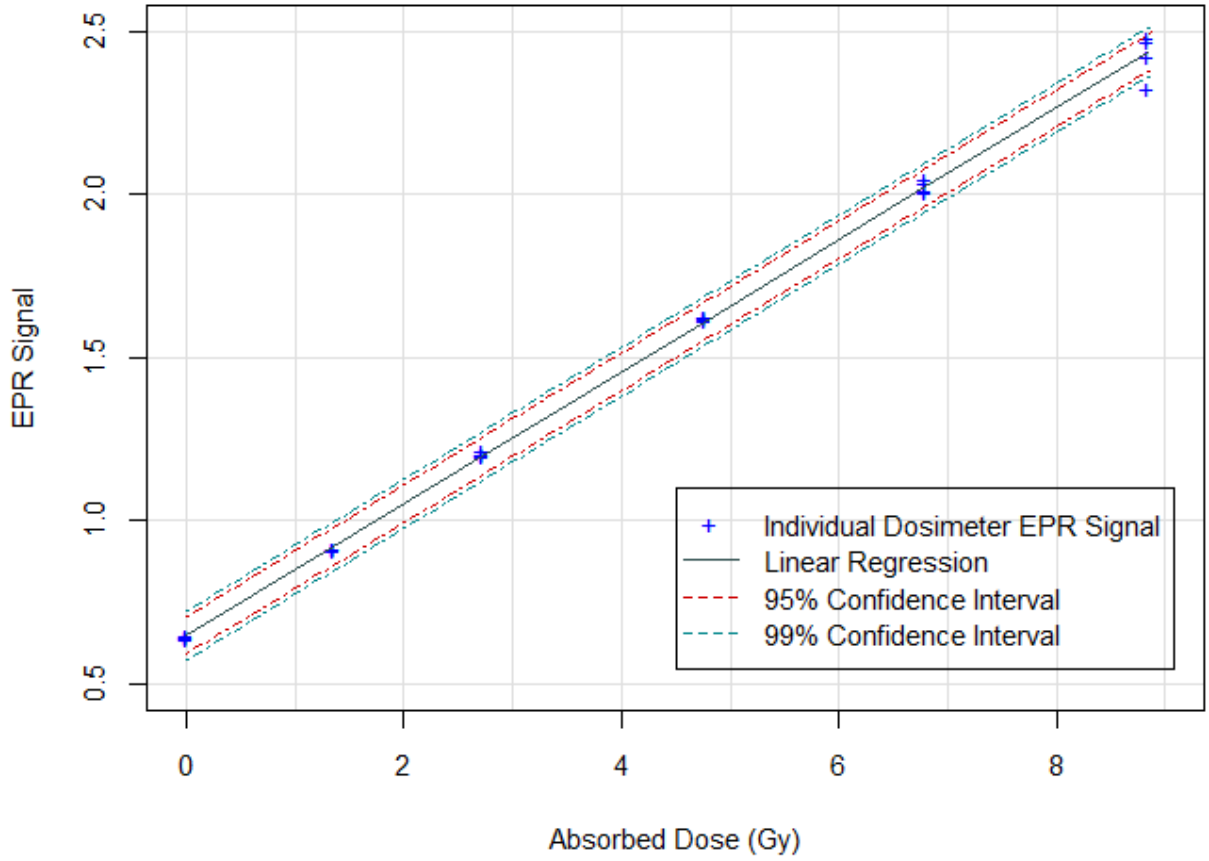

Figure 6.2 - Relation between the absorbed dose from the proton beam by each dosimeter and the respective EPR signal. Each dosimeter signal is represented by the + symbol and the linear model to which the data points were fit to is also visible by the full black line. Considering the uncertainties associated to the obtained regression, the 95 % and 99 % confidence intervals are also plotted and represented by the dashed red and green lines, respectively.

The adjusted R-squared of the model was obtained to verify how well the it fits the data and the result was a coefficient of 0.99 that proves statistically the correlation between both variables.

The residual standard error associated to the regression has the value of 2.9 % which is explained by the uncertainties associated to the EPR signals estimated by the regression. The residual standard error evaluates the differences between the real measured EPR signal of each dosimeter and the estimated signals obtained from Equation 6.1, being considered an estimate of the accuracy of dependent variable.

The individual error (E) associated to each individual signal estimation (S) was calculated for each of the 24 dosimeters using Equation 6.2, considering the EPR signal measured in the spectrometer (S_m).

$$E\ (\%) = \frac{|S_m - S|}{S_m} \times 100 \qquad \text{(Equation 6.2)}$$

This analysis not only confirms how good the regression describes the real data but also allows the verification of whether the residual standard error is a good representative of all dosimeters individual errors or if the regression error is increased by any dosimeter signal whose prediction has a bigger error associated and, consequently has a greater contribution to the increase of the regression residual standard error.

The main analysis to the individual percent errors calculated for every dosimeter are listed in Table ***6.3*** and include the lowest and highest error calculated and also the quantification of the dosimeter signals estimations whose associated errors are below 1 % and 2 %.

Table 6.3 - Summary of the results regarding the error of each signal estimation to each individual dosimeter of the batch. The minimum and maximum percent errors are presented and the amount of estimated signals with associated error (in comparison with the real signals) lower than 1 % and 2 % are counted.

Minimum Error (%)	0.1
Maximum Error (%)	4.8
Number of Estimated Signals with Error < 1 %	$15_{/24}$
Number of Estimated Signals with Error < 2 %	$23_{/24}$

The results confirm that the obtained linear regression allows very accurate predictions of the EPR signals in most cases. In fact, for 15 of the 24 dosimeters the error associated to the signal estimation is lower than 1 % and there is only one situation where the error between the estimated EPR signal and the measured one is bigger than 2 %.

This less exact situation is dosimeter *e*IV – represented by the lower "+" of group 5 – and has an associated error of 4.8 %. This conclusion is a strong indicator that this dosimeter is the one that contributes most to the increase of the residual standard error of the regression.

To verify this, the regression was estimated without dosimeter *e*IV and the residual standard error of the regression was calculated having, as expected, a considerably lower value: 1.4 %. Still, no dosimeter should be removed from the batch and all data must be included in the analysis.

The most important application this test results and of the linear behaviour of the system is regarding the prediction of one either of the variables. With knowledge of the relation between the absorbed dose and the EPR signal it is possible to determine with an associated uncertainty the expected dosimeter EPR signal from their absorbed dose and vice-versa.

In the present case, we take the absorbed dose as a certain value that is considered the same for all the dosimeters of the same group and, thus, all the possible uncertainties are associated to the EPR signals measured. So, considering these uncertainties associated to the predictions made with the linear model, the 95 % and 99 % confidence intervals regarding the EPR signals estimation were obtained.

For the intervals calculation, the parameter used was the residual standard error of the regression and the equation that gives the 95 % confidence interval for the EPR signal ($S_{95\,\%\,CI}$) is Equation 6.3. By calculating this interval for every point of the linear regression, the results falls between the red dashed lines represented in Figure 6.2.

$$S_{95\,\%\,CI} = S \pm 0.057 \qquad \text{(Equation 6.3)}$$

Since the equation of the linear regression to obtain EPR signal does not change and is the base to obtain the confidence intervals, it is expected that the slope of both upper and lower confidence interval equations is the same as the slope of the linear regression to which the confidence interval refers to. Also, coherently with Equation 6.3, the upper and lower lines are symmetrical to the linear regression and represent an interval of amplitude 2 x 0.057 = 0.114.

By observation of Figure 6.2, is possible to see that almost every dosimeter signal is included in the interval and only one – dosimeter *e*IV -, falls outside the interval. This was not very surprising since this dosimeter is the one to which the signal estimation presented the highest error of 4.8 %.

The same calculation was done regarding the 99 % confidence intervals and the conclusions are similar. The equation to obtain this interval for the EPR signal ($S_{99\,\%\,CI}$) is given by Equation 6.4 and, graphically, corresponds to the green dashed lines under and over the linear regression in Figure 6.2.

$$S_{99\,\%\,CI} = S \pm 0.075 \qquad \text{(Equation 6.4)}$$

Again, the slope of both confidence intervals regressions must be the slope of the linear regression of Equation 6.1 and the lines that delimit the interval are also symmetrical to it, having an amplitude of 2 x 0.0751 = 0.150.

The bigger amplitude of the 99 % confidence interval is coherent with statistics because a prediction with higher certainty is associated with a wider confidence interval than an interval predicted with less confidence. Yet, despite the increase of the interval amplitude, dosimeter 24 signal continues to fall out of the interval limits.

Considering Equation 6.3 and Equation 6.4, using only the values of the absorbed doses, taken as certain, the EPR signals associated to each of the doses absorbed by each group and their respective confidence intervals were estimated and shown in Table ***6.4***.

The comparison between these estimations and the real EPR signals has already been made previously and shown to have produced great results. Additionally, since the average group signals are coincident with the linear regression, all the estimations were expected to be very well included in the estimated intervals as the confidence intervals are estimated using as reference the linear regression. So, any divergence would only be expected for some individual dosimeters and not in the average group EPR signals.

Table 6.4 - Estimation of the 95 % and 99 % Confidence Intervals associated to the EPR signals obtained for each irradiated group. No uncertainty is associated to the variable absorbed dose and the confidence intervals were estimated taking into account the uncertainties associated only to the measured EPR signals of each dosimeter in each irradiated group. The amplitude of each confidence interval estimated was also calculated.

Dose (Gy)	Estimated EPR signal	95 % Conf. Interval	99 % Conf. Interval
0.00	0.648	[0.591; 0.705]	[0.573; 0.723]
1.36	0.923	[0.866; 0.981]	[0.848; 0.998]
2.72	1.199	[1.141; 1.255]	[1.123; 1.274]
4.76	1.611	[1.554; 1.668]	[1.536; 1.686]
6.80	2.024	[1.967; 2.081]	[1.949; 2.099]
8.84	2.437	[2.380; 2.494]	[2.361; 2.512]

Practically, if the aim was to predict the EPR signal of a hypothetical dosimeter from the same batch that was known to have absorbed 1.36 Gy from the proton beam it was possible to affirm with 95 % confidence that its signal corrected with the individual calibration factor would be between 0.866 and 0.981 or, in other words, there would only be a probability of 5 % that the dosimeter signal would be outside this interval. Also, there would be only a 1 % probability that the real EPR signal would be

outside the interval [0.848; 0.998]. In case the EPR signal would be outside the expected interval, the dosimeter characteristics should be questioned.

This line of thinking could be applied to predict any dosimeter EPR signal as long as that dosimeter belongs to the original batch and a previous homogeneity evaluation had been made together with the rest of the batch.

However, according to the aim of radiation dosimetry, there is a much bigger interest in being able to predict the absorbed dose rather than EPR signal since this variable can be measured as many times as needed. In this way, with knowledge of the relation between the absorbed dose and the EPR signal (Equation 6.1) and the confidence interval equation for the EPR signal (Equation 6.3 and Equation 6.4), the confidence intervals regarding the absorbed dose can be easily obtained.

Combining Equation 6.1 and Equation 6.3, the 95 % confidence interval for the absorbed dose ($D_{95\,\%\,CI}$) is obtained and presented in Equation 6.5.

$$D_{95\,\%\,CI} = D \pm 0.28 \qquad \text{(Equation 6.5)}$$

Similarly, combining Equation 6.1 and Equation 6.4, the 99 % confidence interval for the absorbed dose ($D_{99\,\%\,CI}$) is obtained and presented in Equation 6.6.

$$D_{99\,\%\,CI} = D \pm 0.37 \qquad \text{(Equation 6.6)}$$

The possibility of being able to predict the absorbed dose from the EPR signal obtained is the most important consequence of the system linearity.

To illustrate the possibility of estimating the absorbed dose from the EPR signal, the average EPR signals of the groups irradiated with the proton beam was used to estimate the absorbed dose with a 95 % and 99 % confidence. This estimation aims to check if the obtained interval would be coincident the real absorbed dose by the groups and to quantify the error associated to the dose estimation.

The results are presented in Table ***6.5*** and the steps followed for the estimation were:

1. Calculation of the estimated dose from Equation 6.1 using the individual EPR signal corrected with the respective individual calibration factor;
2. Calculation of the Absorbed Dose confidence interval from Equation 6.5 (to a 95 % confidence interval) or Equation 6.6 (to a 99 % confidence interval).

Table 6.5 – Estimation of the absorbed dose with a 95 % and 99 % confidence for five groups irradiated with the proton beam considering only their average EPR signal. The dose was estimated for every group and the error associated to that estimated was also calculated. The estimated dose intervals reflect the uncertainties of the linear regression obtained from the measured dosimeter EPR signals and should comprise the real absorbed doses.

Group	Absorbed Dose (Gy)	EPR signal	Estimated Dose (Gy)	Error (%)	95 % Confidence Interval for Dose	99 % Confidence Interval for Dose
a	1.36	0.915	1.32	2.9	[1.04; 1.60]	[0.95; 1.69]
b	2.72	1.206	2.76	1.5	[2.48; 3.04]	[2.39; 3.13]
c	4.76	1.623	4.83	1.4	[4.55; 5.11]	[4.46; 5.20]
d	6.80	2.027	6.83	0.4	[6.55; 7.11]	[6.46; 7.20]
e	8.84	2.427	8.81	0.3	[8.53; 9.09]	[8.44; 9.18]

The errors associated to the estimated doses were calculated using a variation of Equation 6.2 where the real and estimated EPR signals are replaced by the real and estimated absorbed doses. For every group studied the estimated doses are very similar to the real absorbed doses which is confirmed by the low errors associated, always lower than 3 %.

Regarding the confidence intervals, the real absorbed dose values are very well included in the estimated intervals for every group estimation.

Though this analysis was done considering only the average group signals, the estimation process can also be done for every dosimeter and, in this case, only one dosimeter absorbed dose (*eIV*) is not included in the estimated confidence intervals. This situation is not unexpected since it is a consequence of its EPR signal to which the biggest signal estimation error was found, as was already commented previously.

The estimation failure reflects the 5 % and 1 % probabilities of the confidence interval estimation process failing, a situation that is always susceptible to happen.

Ideally, the analysis to the individual dosimeters would produce results as good as the ones obtained in the groups analysis and, to verify this, the errors associated to the dose estimations of each dosimeter were calculated and are presented in Table ***6.6***.

Table 6.6 - Percent errors associated to every dosimeter irradiated with the proton beam dose estimations. The errors account the difference between the real absorbed dose by each dosimeter and the respective value estimated from the linear regression.

Group	Dosimeter I	Dosimeter II	Dosimeter III	Dosimeter IV
a	3.1	4.1	2.2	1.9
b	0.5	0.8	3.5	1.4
c	2.0	1.6	0.8	1.2
d	1.3	1.8	1.1	0.5
e	0.4	2.1	2.8	6.1

Overall, the individual dose estimations are also very satisfactory, within the accepted limits for dose determination in radiotherapy, and the average error is 2.0 %.

A special attention is given, once again, to dosimeter *eIV* but also to dosimeter *aI*, *aII* and *bIII* whose dose estimations are associated to errors bigger than 3 %. Despite these four cases, no error is bigger than 2.9 % which confirms the accurate dose estimations that can be obtained from the signal measured from the lithium formate dosimeters and the system studied.

In this way, it is proved that the method used is trustworthy and can be used for any dose estimation with a considerably high certainty as long as the EPR signal is known and the relation between the absorbed dose and the EPR signal of the respective dosimeter is also well-known.

6.1.3. DISCUSSION

The accurate determination of absorbed doses depends mostly on the dose response of the system and on how well this behaviour can be determined. In this matter, the characteristics of lithium

formate monohydrate have been studied after X-ray irradiations [17, 18] and, regarding its sensitivity, this was considered more advantageous than alanine: not only shown a very linear dose response over a very high dose range as allowed the measurement of doses down to 0.1 Gy. Later, the system was tested for verifications of dose distributions in IMRT and the linear response of the system allowed very accurate dose measurements from 0.2 Gy to 3.5 Gy [19].

Consequently, though no studies had yet been made for proton therapy measurements, the expectations regarding the use of lithium formate dosimeters to achieve high accuracy dose determinations in proton therapy were great.

The obtained results matched the expectations as the residual standard error associated to the linear relation between the absorbed dose and the EPR signal is lower than 3 %. Though no direct conclusions can be taken from this error because it is not associated to the absorbed dose estimation but to the estimation of the EPR signal from the absorbed dose values, its value is a great indicator of the quality of the absorbed doses estimations that will be made considering only the read EPR signal.

Though the absorbed doses were known, the dose estimations procedure was done and the obtained results, in particular the error between the real doses and the estimated ones, were very satisfactory considering the recommended limit of 4 % regarding the dose delivery processes and radiation dosimetry in general [4].

Some cases results were not as great as it would be desirable but no direct explanation was found since the procedure followed was the same for every dosimeter. These situations shows how the system performance can be somewhat unpredictable due to some external factors that may be very difficult to control and that might not have been studied yet. In this way, similarly to what was done regarding photon irradiations [47], it might be interesting to study the influence of factors like the temperature, humidity or light in the dosimeters response after proton irradiations.

Another interesting result is the difference between the average signal of the batch after the Homogeneity Test (0.701) and the average signal of Group *f* in the Linearity Test that absorbed no dose from the proton beam (0.644). Since no extra dose was absorbed, it was expected that the EPR signal would be practically the same. This difference can be partially explained by the fact that the EPR readouts were done in different days and, consequently, were exposed to different spectrometer conditions that might have been more or less stable during the day. Additionally, the dosimeters were exposed to different environmental conditions between their production and each of the readout days which might have contributed to the slightly decrease of the signal.

Though there are no indications that the EPR signal may fade with time after proton irradiation, this option cannot be discarded until the Fading Test is performed. In this way, considering that the time between the proton irradiation and the EPR readout was 7 days due to practical issues, this factor might also have influenced the obtained behaviour increasing the uncertainties within the groups and, consequently, the residual standard error of the regression used to make the dose determinations. Additionally, in case there was indeed some signal fading, this phenomenon may be more noticeable when more radicals are created or, in other words, a bigger dose is absorbed. So, the occurrence of fading that is expected to be more noticeable in higher EPR signals could also explain the biggest standard deviation of Group 5. However, no conclusions can yet be taken regarding this issue.

6.2. BLIND TEST

6.2.1. BATCH HOMOGENEITY ANALYSIS

Twelve dosimeters were produced and the homogeneity test was performed. After the 3 Gy pre-irradiation, each dosimeter was read four times in the spectrometer and the average signals of those measurements are represented by the black circles in represented in Figure 6.3.

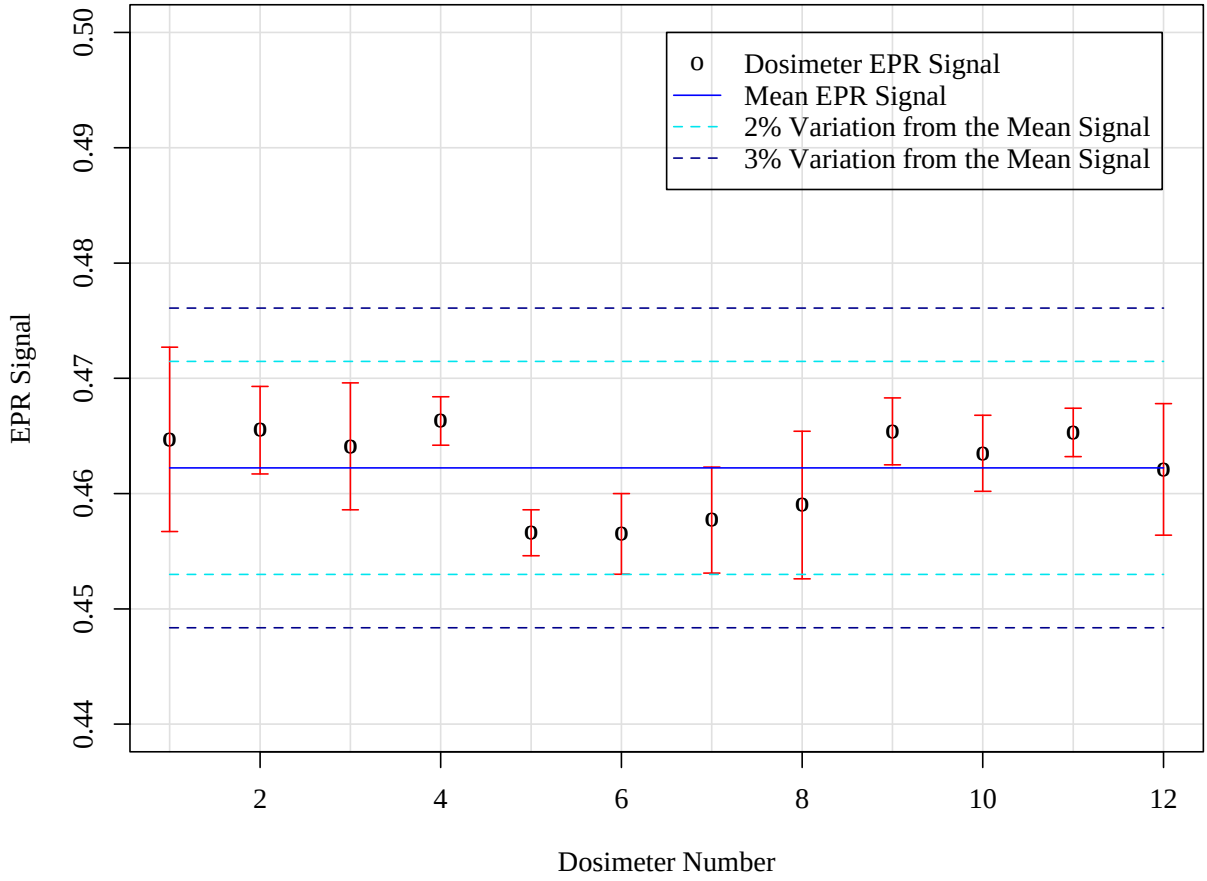

Figure 6.3 – Homogeneity analysis of the batch of dosimeters produced for the Blind Test. The black circles represent each dosimeter EPR signal obtained from the four measurements done and the red error bars represent the biggest deviation from the mean value of those measurements. The light blue and dark blue dashed lines are respectively indicative of the 2 % variation and 3 % variation from the batch EPR signal mean.

A first analysis to Figure 6.3 shows that the EPR signals of the dosimeters after the pre-irradiation of 3 Gy are not very disperse around the mean signal of the batch, represented by the strong blue full line, which is a good indicator regarding the batch homogeneity.

The analysis of the homogeneity begins, however, with the acceptance of the individual dosimeters and, for this, the variation of the values obtained in the four measurements of each dosimeter, shown by the red error bars, are analysed. This statistical measure takes the maximum value of 0.8 % associated to dosimeter 1, which means that all other dosimeters have a lower deviation associated to its measurements.

Supporting this conclusion is the average maximum variation of the four measurements that takes the value of 0.4 % which is a rather small deviation.

Considering all this, is statistically proved that all readings of each dosimeter were quite similar and coherent among themselves and all dosimeters are considered valid.

With all dosimeters accepted to be used, the study regarding the batch homogeneity is made by evaluating the two criteria needed.

To fulfil the first standard, no individual dosimeter should deviate more than 2 % from the mean signal of the batch and conclusions regarding this can be taken by simply observing Figure 6.3 and, more specifically, the limit imposed by the two light-blue dashed lines.

Though the visual analysis is enough to conclude that no dosimeter signal deviates more than 2 % from the mean signal, all signals were analysed individually. With knowledge of the average EPR signal of the batch of 0.462, the 2 % limit signifies that all signals must be included in the interval [0.453; 0.471]. Since this is verified for every dosimeter, the first criteria regarding the homogeneity is fulfilled.

Regarding the second criteria, the relative standard deviation of the batch was calculated and is presented in Table ***6.7*** together with the measures needed to calculate.

Table 6.7 - Overall analysis of the batch to be used in the Blind Test. The quantities average EPR signal, standard deviation of the batch EPR signals and the relative standard deviation of the batch are presented in order to take conclusions regarding the batch homogeneity.

Average Signal	0.462
Standard Deviation (%)	0.4
Relative Standard Deviation (%)	0.8

The relative standard deviation of 0.8 % means the second criteria for homogeneity acceptance that imposes a limit of 1 % for this parameter is achieved. This value also confirms that the EPR signals do not vary much around the batch average signal as it was already evident in Figure 6.3.

In this way, is possible to consider this batch of 12 dosimeters as homogeneous and no corrections to further EPR signals measured with these dosimeters are needed.

6.2.2. BLIND TEST ANALYSIS

After performing the irradiations needed for the present test, each of the dosimeter signals was read four times. Once again, for this analysis, the 3 Gy pre-absorbed by the dosimeters are not accounted in the doses mentioned further that only refer to the dose absorbed during the proton beam irradiations.

As mentioned before, the main purpose of this test is to verify what accuracy is possible to achieve in the determination of the unknown absorbed dose.

The first analysis was regarding the EPR signal of each of the three groups of dosimeters irradiated where the EPR signals of each dosimeter and each group average EPR signal are studied. Also, for each group of dosimeters, the respective standard deviation and relative standard deviation were calculated and all values are presented in Table ***6.8***.

A first look to the results confirms that the unknown dose absorbed by the dosimeters of Group *b* is between the dose absorbed by the other two groups because its average EPR signal is higher than Group *a* EPR signal and lower than Group *c* EPR signal.

Table 6.8 - Summary of the EPR signals measured to the irradiated dosimeters in the Blind Test. The individual EPR signals of every dosimeter are presented together with the respective groups average EPR signal and the associated standard deviation. Also, the relative standard deviation of each group was also calculated to analyse if the measurements were coherent with the groups average.

Group	Absorbed Dose (Gy)	EPR Signal	Average EPR signal	Signal Standard Deviation (%)	Signal Relative Standard Deviation (%)
a	0.00	0.483	0.478	0.6	1.3
		0.472			
		0.483			
		0.475			
b	?	1.545	1.492	5.5	3.7
		1.437			
		1.532			
		1.453			
c	7.90	1.753	1.688	6.5	3.8
		1.666			
		1.726			
		1.606			

The first group (Group *a*) was not irradiated with the proton beam and presented an average signal of 0.478. Since no extra dose was absorbed it was expected that its signal would be similar to the average signal of the batch obtained in the homogeneity test and this was verified.

Regarding the other two groups, the parameter that deserves a bigger attention is the relative standard deviation values that are considerably high. The four readouts of each group were also analysed in Table ***6.8*** and in neither of the groups there is a particular dosimeter whose signal contributes more to the increase of the standard deviation. In fact, observing the four readouts of both groups *b* and *c*, all the four dosimeter signals are well spread around the group average signal that is a good representative of the dosimeters values.

The overall system behaviour is analysed and the relation between the absorbed dose and the EPR signal is obtained considering the data from Group 1 and Group 3.

The dosimeters signals are represented in Figure 6.4 by the blue "+" together with the linear regression that best fit the known data.

For the present batch, the linear relation between the two variables – the EPR signal (S) and the absorbed dose (D) - is given by Equation 6.7.

$$S = (0.153 \pm 0.002) \times D + (0.479 \pm 0.006) \qquad \text{(Equation 6.7)}$$

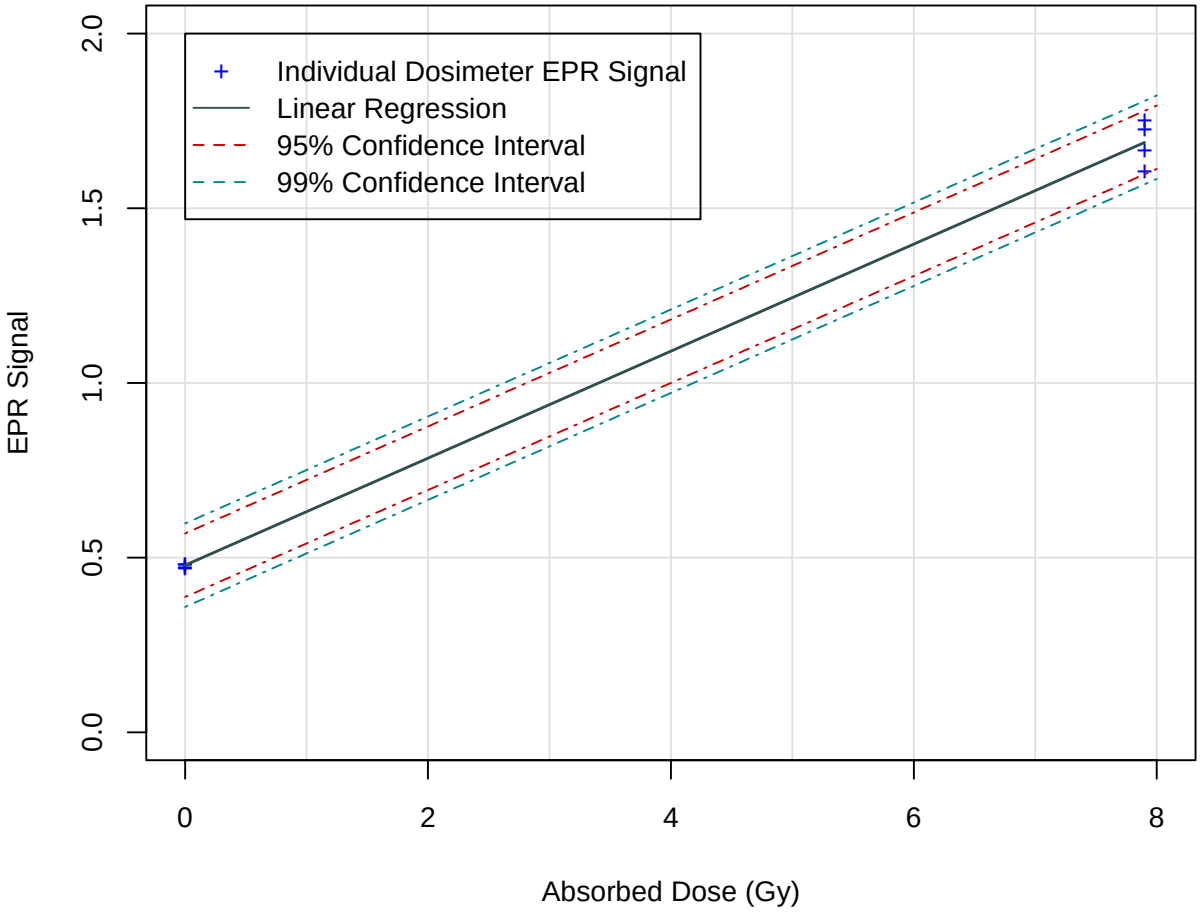

Figure 6.4 - Relation between the absorbed dose by Group 1 and Group 3 dosimeters irradiated in the Blind Test and their respective EPR signal. Each dosimeter signal is represented by the + symbol and the linear model to which the two groups of data points were fit to is shown by the full black line. Additionally, the 95 % and 99 % confidence intervals of the regression are also plotted and represented by the dashed red and green lines, respectively.

The residual standard error associated to the regression is 4.6 % that is explained by the fact that only groups of data points were used to estimate the regression and one of the groups has a big relative standard deviation associated.

Though the estimation of the regression could have been made considering only the groups average signals and the standard deviation values would only be used later for the confidence interval calculations, this would not be representative of the true results obtained and could lead to an inaccurate estimation of the unknown dose. In this way, a bigger margin of error is preferred with the aim of obtaining a better estimation.

Similarly to what was made in the linearity test analysis, the 95 % and 99 % confidence intervals associated to the regression were calculated using as parameter the residual standard error of the regression and these intervals are delimited by the upper and lower red and green dashed lines in Figure 6.4. The 95 % and 99 % confidence intervals of the EPR signal ($S_{95\,\%\,CI}$ and $S_{99\,\%\,CI}$) are given by Equations 6.8 and 6.9, respectively.

$$S_{95\,\%\,CI} = S \pm 0.091 \qquad \text{(Equation 6.8)}$$

$$S_{99\,\%\,CI} = S \pm 0.119 \qquad \text{(Equation 6.9)}$$

However, the main interest is the determination of the absorbed dose from the EPR signal and the confidence intervals associated to the unknown absorbed dose of Group *b*.

To do so, Equation 6.7 was inverted and written in function of the EPR signal, resulting in Equation 6.10.

$$D = (6.54 \pm 0.09) \times S + (-3.13 \pm 0.04) \quad \text{(Equation 6.10)}$$

Additionally, systems of equations were formed using Equations 6.7 and Equation 6.8 to obtain the 95 % confidence interval for the absorbed dose ($D_{95\,\%\,CI}$) and using Equation 6.7 and Equation 6.9 to obtain the absorbed dose 99 % confidence interval ($D_{99\,\%\,CI}$). The resulting equations are, correspondingly, Equation 6.11 and Equation 6.12.

$$D_{95\,\%\,CI} = D \pm 0.59 \quad \text{(Equation 6.11)}$$

$$D_{99\,\%\,CI} = D \pm 0.78 \quad \text{(Equation 6.12)}$$

Due to the high residual standard error of the estimated regression, the confidence intervals for the absorbed doses are a bit larger than what was desired. However, since the relative standard deviation of Group *b* is as high as Group *c* relative standard deviation, it might be convenient to have a wider confidence interval so that all dosimeter estimations might be included in the interval.

Due to the high relative standard of the Group *b* EPR signals it was preferred to use the group average EPR signal to determine the unknown dose of the group and the estimation result is presented in Table ***6.9***. Additionally, the confidence intervals associated to the determined dose were calculated with Equations 6.11 and 6.12.

Table 6.9 - Estimation of the unknown absorbed dose by Group *b* dosimeters. The estimated dose was calculated from the average EPR signal of the group and, concerning this value, the 95 % and 99 % confidence intervals were also calculated and are presented.

Average EPR signal	1.492
Absorbed Dose Estimation (Gy)	6.63
Absorbed Dose 95 % Confidence Interval (Gy)	[6.04; 7.22]
Absorbed Dose 99 % Confidence Interval (Gy)	[5.85; 7.41]

After the estimation made, the unknown dose was revealed by the medical physicist responsible for the irradiations and the absorbed dose by the four dosimeters of Group 2 was 6.70 Gy.

To calculate the error associated to the unknown absorbed dose estimation, Equation 6.2 was applied replacing the signal values for the absorbed dose values. The error between the real absorbed dose and the estimated one is only 1 %, which is a great result associated to a great accuracy.

In this way, despite the bigger relative standard deviations associated to the irradiated groups and the wide confidence intervals obtained, the regression estimated with only two groups of dosimeters led to a quite exact estimation of the dose absorbed by the four dosimeters of the group.

To verify the consequence of the disperse EPR signals of Group *b*, the dose estimation was done for each dosimeter of the group and not the group itself. The estimated doses and the associated estimation errors are presented in Table ***6.10***.

Though the results are not as good as desired, they are coherent with the high relative standard deviation of the group EPR signals and indicate that the, for the present case, the use of individual dosimeters signals for dose determinations might result in very inaccurate estimations. Still, the average of the four dose estimations is still coherent with the value obtained using the average EPR signal.

Table 6.10 – Dose estimations and associate errors of the four dosimeters of Group *b*. The doses were estimated considering the respective EPR signals of the dosimeters and the errors calculated relatively to the real absorbed dose by them.

Dosimeter	**bI**	**bII**	**bIII**	**bIV**
Estimated Dose (Gy)	6.97	6.27	6.89	6.37
Estimation Error (%)	4.0	6.4	2.5	4.9

Several possible justifications for these disperse results are discussed in the next section.

Though more evidences and tests might be needed to confirm the suitability of the lithium formate dosimetry system to measure the absorbed doses, the results obtained are great indicators of the great accuracy that might be reached using the referred system.

6.2.3. DISCUSSION

It is stated that the dose delivery process accuracy should be better than 4 % [4] and research regarding the lithium formate dosimetry system showed that this system can be used for dose determinations within a 2.5 % uncertainty in external beam therapy [19]. Consequently, it was essential to verify the accuracy that could be reached to determine the dose deposited by the clinical proton beam in the lithium formate dosimeters.

Considering the Linearity Test results where the linear dose response of the system was confirmed, the relation between the EPR signal and the absorbed dose was estimated with only two groups of dosimeters. From those groups, only one was irradiated with the proton beam and that same group presented a relative standard deviation associated to the EPR signals considerably high, parameter that also presented a big value for the third group of dosimeters irradiated with the unknown dose. Since this situation only occurs in the groups irradiated with the proton beam, the disperse EPR signals are not likely to be associated with problems in the dosimeters or to the readout process in the spectrometer but, most likely, to the irradiation process.

Despite the irradiation methodology has been followed accurately, the possibility that the dose deposition was not homogeneous is considered. The four dosimeters of each group were placed at the same depth and at the same distance from the centre of the irradiation field but if, for technical reasons, the proton beam deposited its energy in a slightly non-homogeneous way within the irradiation area, the dosimeters absorbed slightly different doses, which justifies the different EPR signals responsible for the bigger relative standard deviation within each group. In this way, a non-homogeneous dose deposition is seen as the likely cause of the disperse results obtained for the two groups irradiated with the clinical proton beam. To correct this in further experiments, the solution might be the rotation of the

phantom 90° after each quarter of irradiation time which results in every dosimeter absorbing the total dose and being exposed to the exact same beam characteristics.

One other top of discussion is the comparison between the regression obtained in the linearity test and in the present test. Ideally, the behaviour would be very similar considering the dosimeters composition and the irradiation set-up but this is not verified. The regressions are different not only in the zero-dose point that depends on the EPR signal of the dosimeters that receive no dose, but also in the slope of the regression that expresses the real relation between the two variables.

The zero-dose point signal is justified by the different signals of the dosimeters after the pre-irradiation for the homogeneity test and, though this value is not coincident, the dose response is not affected by this. The different slope of the regression, however, indicates that the system behaviour is somewhat different and that, at this point, is not possible to generalise the linear regression. Yet, it is believed that this is justified by the small but significant variations of the dosimeters compositions – this batch was considered homogeneous whereas the one used in the linearity test was not -, by the possible instabilities of the spectrometer during the different days of readout but mostly by the fact that the time between the proton irradiations and the EPR readouts was different: 7 days in the Linearity Test and only 1 day in the present test.

Even though no conclusions regarding the signal fading after proton irradiations are yet known, this factor can yet be taken as one of the causes for the different dose response behaviours of the two batches. If so, the hypothesis that the fading behaviour is also different according to the absorbed dose by the dosimeters is placed. According to these specific results, where the slope of the regression whose signals were read one week after the irradiation is bigger than the slope of the regression whose signals were read one day after, it is thought that this possible fading phenomenon is more evident in signals associated to smaller absorbed doses. However, once again, no certainties can be obtained regarding this fading topic.

Despite all this, the main aim of the Blind Test was successfully accomplished and the obtained results are, once again, very promising regarding the possibility to use the lithium formate system for dose measurements with a very reasonable accuracy.

6.3. FADING TEST

6.3.1. BATCH HOMOGENEITY ANALYSIS

A new batch of 25 dosimeters was produced to be used in the fadind characterization. Again, the homogeneity was evaluated considering the same two criteria mentioned in Section 5.

Each dosimeter of this new batch was read four times over the day and the average signal of those four readouts and the maximum deviation from the mean is presented in Figure 6.5 by the black circles and the red error bars, respectively.

Analysing the error bars of each dosimeter, the average maximum deviation from the mean individual signal is 0.7 % and, overall, the four measurements of each dosimeters were very coherent with the biggest deviation associated to their readouts under the 1 % for almost every dosimeter. Only three dosimeters – number 2, 5 and 10 in Figure 6.5 - presented a slightly higher deviation but still lower that 1.1 %. Considering the results, all dosimeters are individually validated and available to be used in the Fading Test.

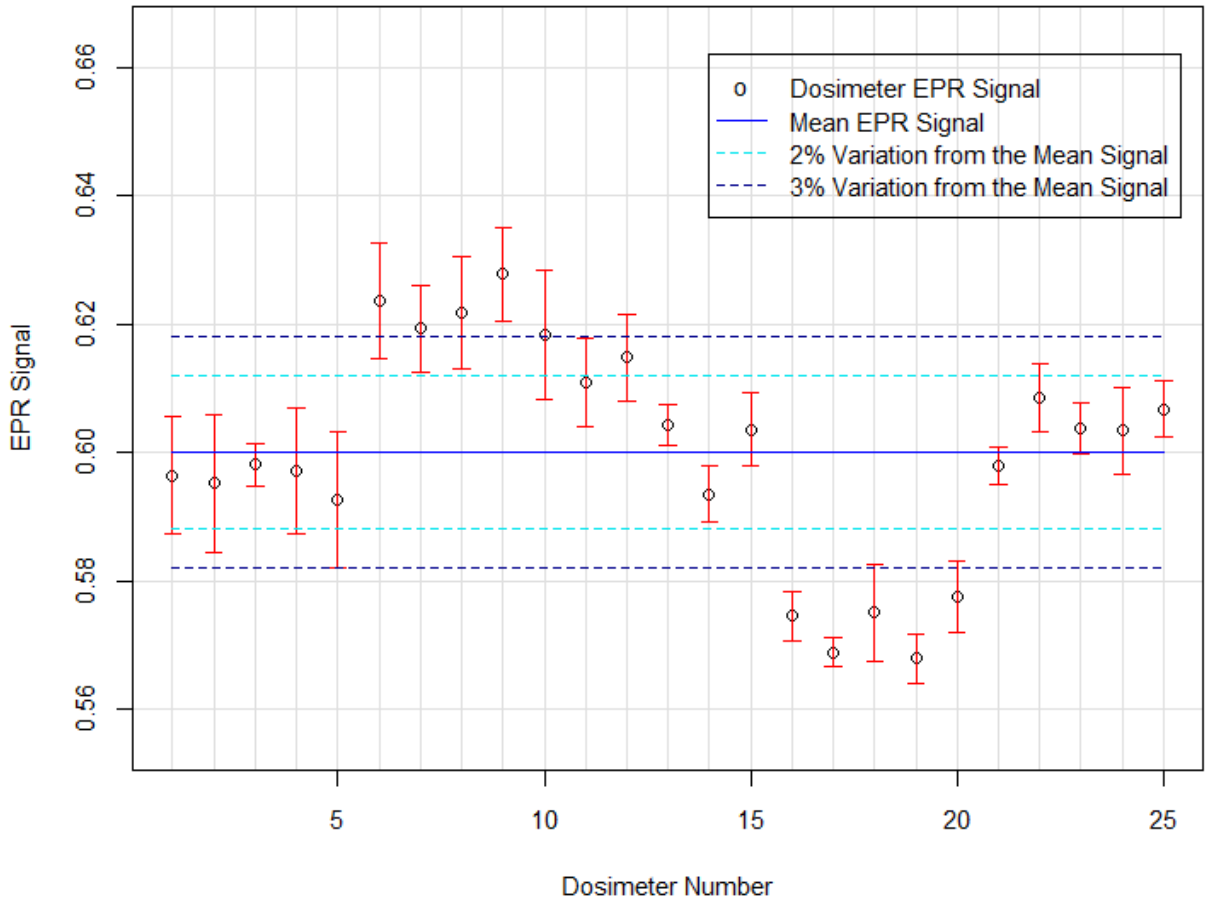

Figure 6.5 – Homogeneity analysis of the batch of dosimeters used in the Fading Test. The circles represent each dosimeter EPR signal obtained from the four measurements done along the day in a rotational schedule and the red error bars represent the standard deviation associated to the four measurements of each dosimeter. The light blue and dark blue dashed lines indicate the 2 % and 3 % variation, respectively, from the whole batch EPR signal mean value (full blue light) that is one of the criteria used to conclude about the homogeneity.

Following the individual analysis, the homogeneity of the batch is studied to verify if the individual calibration factors must be considered or not when the results of the fading test are analysed. This is done by evaluating the same two criteria mentioned in Section 5.

Considering the results, the average signal of the batch – full blue line in the Figure 6.5 – has the value of 0.600 and, regarding the individual dosimeter signal deviation, to agree with the defined variation limit of 2 % from the batch mean signal, no dosimeter average signal should be outside the interval [0.588; 0.612] which does not happen for most dosimeters.

In Figure 6.5 this can be observed and only 14 of the dosimeter signals (56 % of the batch) fall in the space delimited by the light blue dashed lines. Even expanding the deviation limit and analysing the dark blue dashed lines of Figure 6.5, only one other dosimeter is included in the group of dosimeters that deviate less than 3 % from the mean EPR signal of the batch.

This means that some of the dosimeters EPR signals are significantly different from the average signal and, thus, the first criteria regarding the variation of the individual EPR signals is not verified.

Nonetheless, the second condition for the homogeneity verification was simultaneously analysed and the statistical measures needed for that were calculated and are summarized in Table ***6.11***.

For the present batch the relative standard deviation is 2.8 %, considerably higher than the 1 % established for the homogeneity criteria and, consequently, none of the criteria is fulfilled and the batch is not considered homogeneous.

Table 6.11 – Overall analysis of the batch to be used in the Linearity Test. The average EPR signal calculated considering all dosimeters is presented as well as the standard deviation associated to all signals. Also, the relative standard deviation was calculated.

Average Signal	0.600
Standard Deviation (%)	1.7
Relative Standard Deviation (%)	2.8

Yet, all dosimeters were previously considered reliable as individuals and accepted to be used so, to contour the non-homogeneity, individual calibration factors have to be used for further correction of the EPR signals.

6.3.2. FADING ANALYSIS

Once the irradiations were completed, all groups of dosimeters were carried back from SkandionKliniken (Uppsala) to Linköping where all EPR signal measurements were performed in the same day. Each dosimeter signal was read four times in a rotating schedule and its individual signal was obtained as the average of those four measurements.

The absorbed doses mentioned in this section only refer to the ones received by the clinical proton beam and do not account the 3 Gy pre-absorbed in the homogeneity test. Additionaly, the EPR signal values presented already account the ICF correction.

The first analysis made was regarding each of the irradiated groups and the main results are presented in Table ***6.12***.

Table 6.12 - Summary of the measured EPR signals to each of the groups irradiated over the weeks in the Fading Test. For each group the average signal of the four dosimeters belonging to the respective group is presented as well as the associated standard deviation and relative standard deviation. In addition, all groups' signals were normalized to the last group irradiated - Group *f* to calculate the relative EPR signal and, from this value, the percentage of the occurred fading was also calculated.

Group	Days after Irradiation	Average EPR signal	Standard Deviation (%)	Relative Standard Deviation (%)	Relative EPR Signal	Fading (%)
f	2	2.077	2.3	1.1	1.000	0.0
e	3	2.075	4.3	2.1	0.999	0.1
d	10	2.010	1.7	0.8	0.968	3.2
c	17	1.996	2.6	1.3	0.961	3.9
b	24	1.943	2.1	1.1	0.935	6.5
a	31	1.944	5.7	2.9	0.936	6.4

For each group the average EPR signal was calculated as well as the standard deviation and the relative standard deviation associated to the four dosimeters of each group. Also, considering the last group irradiated as the reference group to which highest EPR signal measured is associated, all the average signal groups were normalized with respect to that group. To calculate the relative EPR signals for each group ($S_{Rel\ i}$), Equation 6.13 was used.

$$S_{Rel\ i} = \frac{S_{\ Group\ i}}{S_{\ Group\ f}} \qquad \text{(Equation 6.13)}$$

Additionally, the relative EPR signal can also be used to quantify the fading that has occurred. So, using Equation 6.14, the values of the average fading that occurred in each group ($F_{\ Group\ i}$) were calculated and are also presented in Table ***6.12***.

$$F_{\ Group\ i}\ (\%) = (1 - S_{Rel\ i})\ \times\ 100 \qquad \text{(Equation 6.14)}$$

In both Equations 6.13 and 6.14, the variable $S_{Rel\ i}$ corresponds to the average relative signal of the group i to which the relative signal or the fading are being calculated.

From the results, there is a decrease of the relative EPR signal as the time between the irradiation and the readout increases or, in other words, an increase of the signal fading.

Regarding the relative standard deviation of each group, the values vary quite randomly and this change does not appear to be related with the time after irradiation but to some other factors like, for example, the spectrometer instabilities or the fact that, during the irradiation process, the dosimeters might not have absorbed the exact same dose.

Considering the relative signal, during the 31 day period, there was a maximum fading of 6.5 % associated to the dosimeters of Group *b*, slighly higher than the fading of 6.4 % associated to Group *a* – the first to be irradiated. Yet, it is not certain that the fading was higher in Group *b* dosimeters due to the higher relative standard deviation associated to Group *a* EPR signals which indicated that it might exist one or more dosimeters in that group that vary considerably from the others and that may be leading to an misrepresentative increase or decrease of the average signal. The same situation might also occur with group *e* that has a relative standard deviation of 2.1 %.

For the remaining groups, the relative standard deviation is no bigger than 1.3 % indicating that the dosimeters signals within those groups do not vary much from the calculated average signal and, therefore, that average signal of the group is a good representative of the signals of the respective individual dosimeters.

The small variations in the dose absorbed by each group of dosimeters in the successive weeks were not corrected for the following study of the fading process because the dose response of the system was not studied for the present batch of dosimeters and, has it was verified previously, the dose response behaviour may vary slightly from batch to batch. Either way, the absorbed dose difference are quite small and can be considered negligible.

With this in mind, to verify how the individual relative signals within each group vary and to get a general view of the relation between this variable and the time after the group irradiation, all the relative signals are presented in Figure 6.6.

The dosimeters relative signals are represented by the "+" symbol and the regression to which they were best fit into is represented by the dark full line. The represented regression approximately goes through each of the groups average signal so it is easy to take conclusions on how well the average group signals represent the individual EPR signals belonging to that same group.

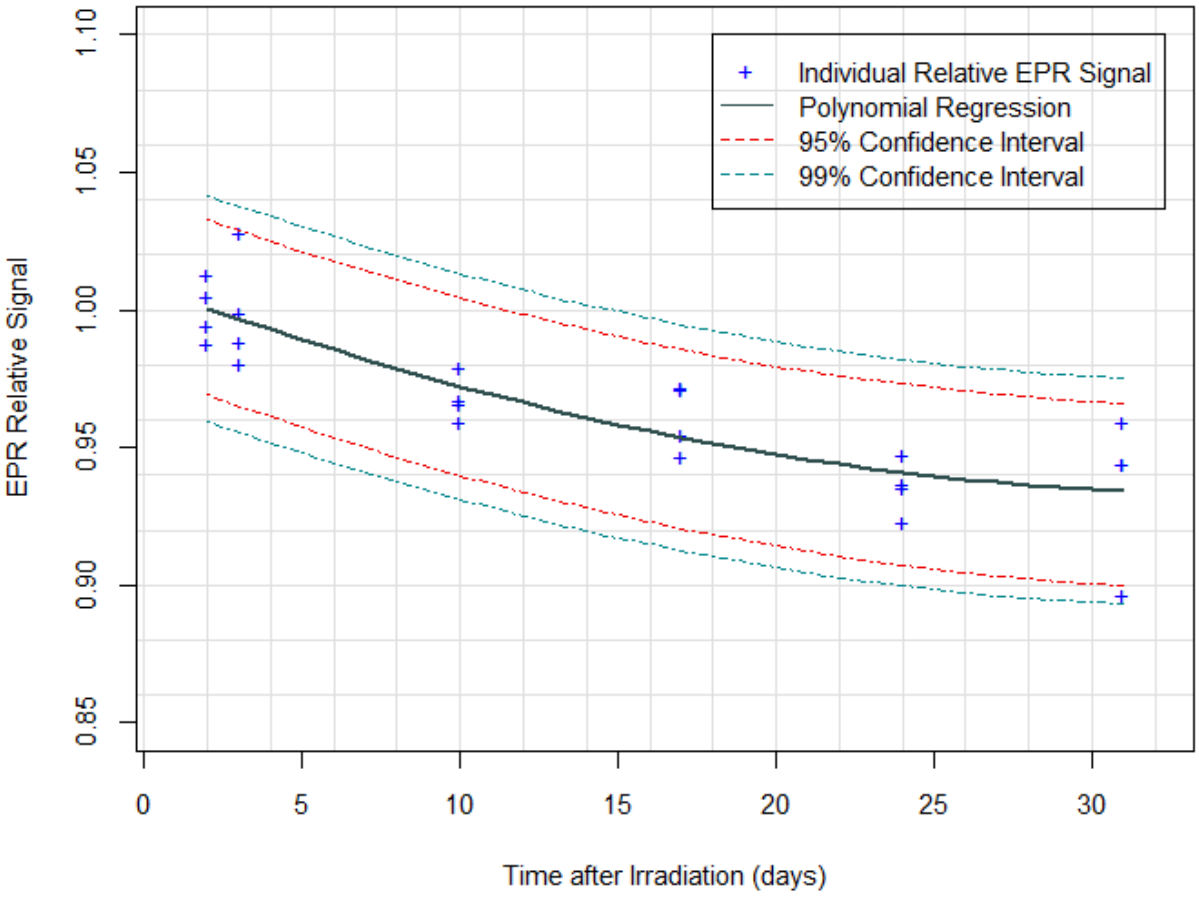

Figure 6.6 - Relation between the relative EPR signal of the dosimeters and the time between irradiations and signal measurement. Each dosimeter signal is represented by the + symbol and the best fitting regression model is represented by the full dark line. Considering the uncertainties associated to that regression, the 95 % and 99 % confidence intervals are also plotted by the dashed red and green lines, correspondingly.

It is possible to identify easily each irradiated group by the four "+" symbols vertically aligned over the respective time after irradiation and, from the left to the right, the groups correspond to Group f, Group e, Group d, Group c, Group b and Group a.

For most groups, the dosimeters signals are close and well spread around its mean value and the regression is a good representative of the relative EPR signals obtained in those groups. However, for other groups the dispersion is visibly bigger, which is coherent with the group analysis previously made, where the possibility that there was one or more dosimeters signals deviating more from the others in Group e and Group a was placed.

Also coherently with the group analysis, Figure 6.6 expresses in a very clear way the appearant relative signal decrease as the time between the irradiation and the signal readout increases.

The observed fading is very well supported by the polynomial regression, given by Equation 6.15, that best fits the experimental data. This regression considers the time after irradiation (d) as the dependent variable that can be used to predict the relative signal (S_{rel}) of any dosimeter.

$$S_{rel} = (6.012 * 10^{-5})\, d^2 - (4.275 * 10^{-3})\, d + 1.009 \qquad \text{(Equation 6.15)}$$

The correlation between the two variables is given by the adjusted R-squared, which was calculated and takes the value of 0.723. Though most of the data points are well represented and fall near the regression, following the polynomial behaviour and supporting the relation between the fading increase over the time, some data points fall quite far from the estimated regression and, consequently,

the R-squared value is not as close to 1 as it would be desired. Either way, overall, the regression can explain most of the observed data variability and the relation between the time after the irradiation and the obtained relative signal is clear.

Considering the existence of signal fading and the period of two days between the last irradiation day and the EPR readouts day, it is likely that a minimal fading have occurred during this period and this can also be considered if signal corrections regarding the signal fading are ought to be done. From Equation 6.15, the relative signal associated to the irradiation day was estimated and takes the value of 1.009, which indicates that there was a 0.9 % fading between day 29 – last irradiation day - and day 31 – EPR readouts day. Yet, for the present analysis this will not be accounted because it is a estimation and not real data measured.

Any estimation has an uncertainty associated due to the EPR signal uncertainties and due to the residual standard error of the regression used and the residual standard error of the regression quantifies the residuals between the values estimated by the regression and the real obtained values. For the present regression it takes the value of 1.6 % which is a very optimistic result.

A more detailed analysis was made to calculate the individual estimation errors associated to every dosimeter susing Equation 6.2. As mentioned before, this quantity evaluates the difference between the measured relative EPR signal and the estimated ones by the obtained regression for each individual case, comparatively to the first. The main analysis to the individual percent errors calculated is listed in Table ***6.13***.

Table 6.13 - Summary of the results regarding the error of the relative signals estimation for every dosimeter. The minimum and maximum percent errors are presented and the amount of estimated signals with associated error lower than 1 % and 2 % (in comparison with the measured signals) are counted.

Minimum Error (%)	0.1
Maximum Error (%)	4.2
Number of Estimated Signals with Error < 1 %	$12_{/24}$
Number of Estimated Signals with Error < 2 %	$21_{/24}$

For half of the dosimeters of the batch, the error between the real relative signal and the estimated value by the regression is lower than 1 %. When considering a maximum error of 2 % for the estimation, 21 of the total 24 dosimeters fulfil the criteria. So, coherently with the small residual standard error associated to the regression, it is now verified that most of the point estimations have, in fact, a considerably low percent error associated which is a great indicator of the accuracy of the estimations to be made.

The three dosimeters whose estimation errors are bigger than 2 % can be easily identified in Figure 6.6 and correspond to the dosimeters signals that fall more far from the regression line: one belonging to group *e* and two dosimeters belonging to group *a*. In fact, it was already expected that the situations to which the regression would produce less accurate estimations would be associated to any dosimeter from the groups with the highest relative standard deviations in Table ***6.12***.

Making the association with the dosimeters in Figure 6.6, the highest estimation errors are:

- 2.6 % - dosimeter represented by the highest "+" of group *a*
- 3.1 % - dosimeter represented by the highest "+" of group *e*
- 4.2 % - dosimeter represented by the lowest "+" of group *a*

Despite these situations whose relative signals vary considerable from the other dosimeters of the respective groups, their EPR signals are still valid and must be considered in the analysis.

The direct application of this test is the possibility to predict how much a dosimeter EPR signal has faded in a certain period of time so that, as a consequence, the EPR signal associated to the irradiation day can be calculated and the initial absorbed dose can be accurately estimated. In this way, it is important to estimate the confidence intervals regarding the relative signals estimations and the fading estimations.

Considering the residual standard error associated to the estimated polynomial regression, the 95 % confidence interval of the relative EPR signal ($S_{Rel\,95\,\%\,CI}$) that is delimited by the red dashed lines in Figure 6.6 is expressed in Equation 6.16.

$$S_{Rel\,95\,\%\,CI} = S_{Rel} \pm 0.031 \qquad \text{(Equation 6.16)}$$

The confidence interval associated to the fading percentage ($F_{95\,\%\,CI}$) was obtained by combination of Equation 6.13 and Equation 6.15 and is presented in Equation 6.17.

$$F_{95\,\%\,CI}\,(\%) = F\,(\%) \pm 3.1 \qquad \text{(Equation 6.17)}$$

So, the 95 % confidence interval produces fading estimations with an uncertainty of 3.1 %. With an analysis of Figure 6.6, is possible to conclude that almost every dosimeter relative signal is well included in the interval and there is only one situation that falls outside the 95 % confidence interval. This is the dosimeter represented by the lowest "+" of Group *a* – read 31 days after the irradiation – and to which the highest estimation error was associated.

The same line of thinking was applied to obtain the 99 % confidence interval of the relative EPR signal, represented by the green dashed lines of Figure 6.6. The 99 % confidence interval equations of the relative signal ($S_{Rel\,99\,\%\,CI}$) and the fading ($F_{99\,\%\,CI}$) are Equation 6.18 and 6.19, respectively.

$$S_{Rel\,99\,\%\,CI} = S_{Rel} \pm 0.041 \qquad \text{(Equation 6.18)}$$

$$F_{99\,\%\,CI}\,(\%) = F\,(\%) \pm 4.1 \qquad \text{(Equation 6.19)}$$

An estimation with 99 % certainty results in an interval of amplitude 8.2 % that is a range much wider than what was desired to be considered meaningful. This amplitude is bigger than the maximum fading of 6.50 % registered for Group *b* which means that the estimated confidence intervals limits will be too wide and might lead to erroneous conclusions.

To analyse the fading estimations and the respective 95 % and 99 % confidence intervals obtained from Equations 6.15, 6.14, 6.17 and 6.19, calculations regarding the time intervals studied in the test were made and are presented in Table ***6.14***. No fading estimation was done regarding the reference group and the inferior limit of the intervals was set as 0 because any negative value means that no fading occurred.

The main problem associated to the wide confidence intervals is that, for example, a fading estimation of 2.8 % (associated to a time of 10 days between the irradiation and the readout) is easily included in the 95 % confidence interval calculated for 3, 10 or 17 days. If the 99 % interval is considered, the estimation is included in all the intervals estimated. However, considering that the confidence intervals are used to include all possible abnormal fading situations, the wide range of the intervals is also considered as an advantage.

Table 6.14 - Fading estimations, in percentage, associated to the days studied in the Fading Test with the calculation of the respective confidence intervals. The estimations were done considering only the time between the irradiation and the EPR readout using the fading regression equation. Additionally, for each estimation, the 95 % and 95 % Confidence Intervals were also calculated for the signal fading.

Time after Irradiation	Fading Estimation (%)	95 % Confidence Interval (%)	99 % Confidence Interval (%)
3	0.3	[0; 3.4]	[0; 4.4]
10	2.8	[0; 5.9]	[0; 6.9]
17	4.6	[1.5; 7.7]	[0.5; 8.7]
24	5.9	[2.8; 9.0]	[1.8; 10.0]
31	6.6	[3.5; 9.7]	[2.5; 10.7]

6.3.2. DISCUSSION

Many attempts have been made over the last years to determine a possible signal fading in lithium formate dosimeter however, evidences that the EPR signal from lithium formate is stable during at least one month after photon irradiations were provided recently [47].

Concerning proton beam irradiations, no studies focused on the signal fading in lithium formate dosimeters had yet been made. Though, some studies concerning the fading in alanine were done. In this topic, the study of the occurrence of decay in free-radical concentrations in alanine after high-LET irradiation stated that a considerable decay was observed after dose depositions from heavy charged particle beams and that a bigger decay was found for higher LET radiation [22].

Also, about the lithium formate system performance after proton irradiations, research indicated that the interactions between proton radiation and matter were responsible for a lower EPR signal in comparison to the EPR signal obtained after photon irradiations [23]. In the tracks of densely ionizing particles, where the energy is deposited in the track at doses above saturation for radical production, the rate of radical recombination's is thought to be considerably bigger and, consequently, explains the lower signal obtained.

The results obtained in the Fading Test are obviously coherent with the previous researches because they confirm that after a heavy charged particle irradiation – using protons – there is in fact a non-negligible signal decay.

This fading appears to be bigger in the first days after the irradiation and then, as the days go by, the fading rate appears to stabilize. As the fading in the signal of heavy particles is attributed to the radical recombination, an exponential decay of the signal would be expected. Yet, for the one month period tested, the polynomial regression was the one that best represented the data obtained.

According to studies made previously, it is believed that when increasing the experiment time and obtaining more data points, this exponential behaviour will become clear and the estimated regression will be used in any situation.

Consequently, to confirm the fading behaviour more tests regarding this issue need to be done. Not only the repetition of the present test but also and the extension of the experiment duration to 3 or

4 months, in which the regression best fitting the data is expected to be an exponential regression. The possibility to repeat the signals readouts 30 and 60 days after the first readout day was placed, however that would insert one additional variable in the readout process and this would not be consistent with the methodology followed in this test.

The experimental method used in the Fading Test based on several irradiations at different time intervals and only one readout started to be preferred in recent studies [19, 20, 21] because the absence of a reference sample allows a narrower sweep width[7] of the EPR spectrum and thus more sampling points concentrated over the signal of interest with a lower uncertainty associated. By performing two readouts in different days a reference sample would be needed and the uncertainties would be bigger.

Since the existence of signal fading after proton irradiation is validated, one factor that gains importance and need to be considered in further studies is the time between the irradiations with the proton beams and the EPR signal measurements. Ideally, the EPR signals should have been read immediately after the last irradiation but, since the irradiation facilities and the EPR spectrometer equipment are located in different cities[8], this is still not possible and the best solution is to perform the signal measurements in the day after the irradiation.

Contrarily to what was found for the lithium formate dosimeters signal after photon beam irradiations, the signal upcoming the dose absorption from a clinical proton beam is less stable and decreases slightly with time. The most important application of knowing the fading behaviour is the possibility to estimate accurately the EPR signal that the dosimeter would present if the readout was done in the same day of the irradiation and, from EPR value and knowing the dose response of the dosimetry system, estimate accurately the dose absorbed by the dosimeter.

[7] measure of the width of the frequency spectrum to be analysed

[8] The time travel between Uppsala and Linköping in no less than 3 hours

Chapter 7

CONCLUSIONS AND FUTURE WORK

The lithium formate EPR dosimetry system has been developed and methodically characterized regarding its performance in proton therapy dose verifications.

With all results analysed, the system in study is considered a very promising tool for several proton radiation dosimetry purposes not only because of its robustness but also for allowing very accurate radiation dose measurements, with uncertainties under the limit accepted in dose delivery processes. Nevertheless, contrarily to what was verified in the lithium formate system tests with photon radiation where no signal fading exists nor temperature dependence, more factors appear to influence the system behaviour when the radiation dose is delivered by a proton beam. So, a greater attention shall be given to these factors to optimize the lithium formate system utilization.

One certainty of the characterization is the linear relation between the absorbed dose and the EPR signal for doses between 0 and 9 Gy, commonly used in radiotherapy, and the fact that this relation can be accurately estimated with only two groups of data points. The second main conclusion is the occurrence of fading of the EPR signal of the dosimeters with time when the dose is absorbed from heavy charged particles like protons.

Regarding the proton irradiations, the dose was delivered in only one irradiation similarly to what was done in the system tests with photon beam irradiations. However, this resulted in noticeable EPR signal differences among the dosimeters irradiated which was justified with a non-homogeneity of the proton dose delivered throughout the irradiation field. In this way, as the proton beam is not as homogeneous as the photon beam, for further tests with proton beams it is advised to rotate the phantom 90° after each quarter of the total irradiation time so that each dosimeter is exposed to the exact same irradiation characteristics.

Moreover, considering all results obtained, the use of one group only pre-irradiated with photon radiation as the zero-dose point group for the calibration regression estimation is questioned. Unless the EPR signal is read right after the proton irradiation, all dosimeters irradiated with protons are likely to experience some fading resulting in lower EPR signals in comparison to the real EPR signals associated to the respective absorbed doses, while the group only pre-irradiated in the homogeneity test does not experience any fading. So, this variable must be eliminated and all groups must be exposed to the proton beam, even if the absorbed dose by the zero-dose group is minimal. Once the fading behaviour is established by more tests similar to the one made in this project, a fading correction can be introduced

and the signals from the dosimeters irradiated only with photons can be corrected as if they had experienced some fading.

So, the fading phenomenon gains a huge importance if the best performance of the lithium formate EPR dosimetry system in proton radiation clinical verifications is wanted. Not considering the existence of fading, the measured EPR signals may not correspond to the real EPR signal – right after the irradiation – and, consequently, erroneous conclusions about the absorbed dose might be taken. Consequently, this phenomenon must be fully understood an to do so, a deeper investigation regarding the fading process is required in the future.

According to previous studies, the existence of fading is justified with the radical recombination that is characterized by an exponential behaviour. Though this was not the obtained regression in the Fading Test, an exponential behaviour is expected if a longer period is analysed. So, for a fully characterization of the fading process, it is of the utmost importance to repeat this investigation, test the fading behaviour for different absorbed doses, extend the experiment to at least 3 to 4 months and verify if it is possible to generalize the fading behaviour to all lithium formate dosimeters.

With all these factors considered the performance of the lithium formate system will certainly be improved and lead to even better and more accurate results. So, other tests and applications can and should be considered.

As important as the characterization of the system is the verification of its suitability to determine the absorbed doses in points at different depths and under different materials similar to the human body tissues – different stopping power ratios -, to simulate measurements within the human body, the main purpose of radiation dosimetry in radiotherapy.

These tests already started to be planned but no accurate conclusions can be taken until the stopping power ratio of the lithium formate dosimeters in proton irradiations is known (and consequently the water to tissue equivalence of the material), so that the results can be compared with Monte Carlo simulations or with the results obtained by the ionization chamber. Until this moment, due to the non-existence of information regarding the stopping power ratio of lithium in proton beams and due to the small dimensions of the dosimeters created, it was not possible to calculate the wanted quantity either theoretically or experimentally. Thus, the determination of the stopping power ratio in proton beam irradiations of the lithium formate mixture used to produce the dosimeters is one of the priorities before further tests with these dosimeters shall be made.

Despite the need to make dose verifications is human phantoms, the lithium formate EPR technique is not being developed as an alternative dosimetry systems used for daily purposes but to other applications where the high accuracy and precision of the measurements are prioritized and, in this matter, the presented system might become one of the best options available.

Tough the readout process is quite time consuming and the result is not presented directly, this system was shown to have a linear dose response over large dose ranges and over the ranges used in radiotherapy procedures and for allowing the EPR signal reading multiple times without any consequence for the dosimeter or the signal itself. These are clear advantages over other passive dosimeters like the ones used in thermoluminescence dosimetry. Additionally, contrarily to ionization chamber dosimetry, no connecting cables are required so the dosimeters can be used for various measurement situations without being influence by the beam direction.

The other great advantage to some of the other dosimetry techniques is the possibility to use tissue equivalent materials as the dosimeter material. In particular, the choice of using lithium formate as the dosimeter material, a material with scattering and absorption properties very equivalent to the body tissues properties, allows more accurate and precise measurements of the absorbed doses in radiation qualities different from the radiation quality used for calibration of the dosimetry system.

With the research developed in the present dissertation, the great expectations for the lithium formate EPR dosimetry system were corresponded and, though more research still needs to be done regarding its use for proton beam dose verifications, there is no doubt that the dose measurements performed with this system are of great accuracy and precision. So, this alternative dosimetry system is a very promising tool for the verification and increase of the precision with which the dose is delivered to the patients in radiation therapy and also in proton therapy, approaching the main aim of radiation dosimetry.

BIBLIOGRAPHY

[1] B. W. Stewart and C. P. Wild, "World Cancer Report 2014," International Agency for Research on Cancer, 2014.

[2] National Cancer Institute, "NIH: National Cancer Institute," June 2010. [Online]. Available: https://www.cancer.gov/about-cancer/treatment/types/radiation-therapy/radiation-fact-sheet#q1. [Accessed November 2016].

[3] M. Goitein, Radiation Oncology: A Physicist's-Eye View, New York: Springer-Verlag New York, 2008.

[4] A. Lund and M. Shiotani, Applications of EPR in Radiation Research, Springer, 2014, pp. 509-538.

[5] B. J. McParland, Medical Radiation Dosimetry: Theory of Charged Particle Collision Energy Loss, 1 ed., Springer-Verlag London, 2013, pp. 3-64.

[6] E. B. Podgorsak, Radiation Oncology Physics: A Handbook for Teachers and Students, Vienna: International Atomic Energy Agency, 2005, pp. 71-98.

[7] T. Rivera-Montalvo, "Radiation Therapy Dosimetry System," *Applied Radiation and Isotopes*, vol. 83, pp. 204-209, 2014.

[8] International Atomic Energy Agency, "Use of paramagnetic electron resonance dosimetry with tooth enamel for retrospective dose assessment," International Atomic Energy Agency, Austria, 2002.

[9] K. Mehta and R. Girzikowsky, "Alanine-ESR Dosimetry for Radiotherapy IAEA Experience," *Applied Radiation and Isotopes*, vol. 47, no. 11/12, pp. 1189 - 1191, 1996.

[10] R. D. Adams, "The Future of Medical Dosimetry," *Medical Dosimetry*, pp. 159-165, 2015.

[11] T. Kron, "Medical Radiation Dosimetry: Concepts and Needs," *AIP Conference Proceedings*, vol. 1345, no. 1, pp. 24-35, 2011.

[12] W. W. Bradshaw, D. G. Cadena, G. W. Crawford and H. A. W. Spetzler, "The use of Alanine as a Solid Dosimeter," *Radiation Research*, vol. 17, no. 1, pp. 11-21, 1962.

[13] D. F. Regulla and U. Deffner, "Dosimetry by ESR Spectroscopy of Alanine," *Applied Radiation and Isotopes,* vol. 33, no. 11, pp. 1101 - 1114, 1982.

[14] O. Baffa and A. Kinoshita, "Clinical applications of alanine/ electron spin resonance dosimetry," *Radiation and Environmental Biophysics,* vol. 53, pp. 233-240, 2014.

[15] A. Bartolotta, B. Caccia, P. L. Indinova, S. Onori and A. Rosati, "Applications of alanine-based dosimetry," in *International symposium on High-dose dosimetry,* Vienna, 1985.

[16] A. Lund, S. Olsson, M. Bonora, E. Lund and H. Gustafsson, "New materials for ESR dosimetry," *Spectrochimica Acta Part A,* pp. 1301-1311, 2002.

[17] T. A. Vestad, E. Malinen, A. Lund, E. O. Hole and E. Sagstuen, "EPR dosimetric properties of formates," *Applied Radiation and Isotopes,* vol. 59, pp. 181-188, 2003.

[18] E. Lund, H. Gustafsson, M. Danilczuk, M. D. Sastry, A. Lund, T. A. Vestad, E. Malinen, E. O. Hole and E. Sagstuen, "Formates and dithionates: sensitive EPR-dosimeter materials for radiation therapy," *Aplied Radiatin and Isotopes,* pp. 317-324, 2005.

[19] H. Gustafsson, E. Lund and S. Olsson, "Lithium formate EPR dosimetry for verifications of planned dose distributions prior to intensity-modulated radiation therapy," *Physics in Medicine and Biology,* pp. 4667-4682, 2008.

[20] L. Antonovic, H. Gustafsson, G. Alm Carlsson and Å. Carlsson Tedgren, "Evaluation of a lithium formate EPR dosimetry system for dose measurements around Ir-192 brachytherapy sources," *Medical Physics,* vol. 36, pp. 2236-2247, 2009.

[21] E. Adolfsson, G. Alm Carlsson, J. E. Grindborg, H. Gustafsson , E. Lund and Å. Carlsson Tedgren, "Response of lithium formate EPR dosimeters at photon energies relevant to the dosimetry of brachytherapy," *Medical Physics,* vol. 37, pp. 4946-4959, 2010.

[22] E. Waldeland, E. O. Hole, B. Steberlöw, E. Grusell, E. Sagstuen and E. Malinen, "Radical Formation in Lithium Formate EPR Dosimeters after Irradiation with Protons and Nitrogen Ions," *Radiation Research,* vol. 174, pp. 251-257, 2010.

[23] J. M. Hansen and K. J. Olsen, "Predicting decay in free-radical concentration in L-A-alanine following high-LET radiation exposures," *Applied Radiation and Isotopes,* vol. 40, pp. 935-939, 1989.

[24] M. Marrale, A. Carlino, S. Gallo, A. Longo, S. Panzeca, A. Bolsi, J. Hrbacek and T. Lomax , "EPR/ alanine dosimetry for two therapeutic proton beams," *Nucelar Inst. and Methods in Physics Research,* pp. 96-102, 2016.

[25] E. Adolfsson, "Lithium formate EPR dosimetry for accurate measurements of absorbed dose in radiotherapy," Linköping University Medical Dissertations, Linköping, 2014.

[26] A. Ableitinger, S. Vatnitsky, R. Herrmann, N. Bassler, H. Palmans, P. Sharpe , S. Ecker, N. Chaudhri, O. Jakel and D. Georg, "Dosimetry auditing procedure with alanine dosimeters for light ion beam therapy," *Radiotherapy and Oncology,* vol. 108, pp. 99-106, 2013.

[27] E. Adolfsson, H. Gustafsson, E. Lund, G. Alm Carlsson, S. Olsson and Å. Carlsson Tedgren, "A system for remote dosimetry audit of 3D-CRT, IMRT and VMAT based on lithium formate dosimetry," *Linköping University Electronic Press,* 2014.

[28] J. Cameron, "Radiation Dosimetry," *Environmental Health Perspectives,* vol. 91, pp. 45-48, 1991.

[29] S. Kumar, "Second Malignant Neoplams Following Radiotherapy," *International Journal of Environment Research and Public Health,* vol. 9, pp. 4744-4759, 2010.

[30] S. Yajnik, Proton Beam Therapy: How Protons are Revolutionizing Cancer Treatment, New York: Springer, 2013.

[31] A. Lund and M. Shiotani, Applications of EPR in Radiation Research, Springer International Publishing, 2014, pp. 509-538.

[32] L. D. Skarsgard, "Radiobiology with heavy charged particles: a historical review," *Medical Physics,* pp. 14:1-19, 1998.

[33] M. Jermann, "Group, Particle Therapy Co-Operative," November 2016. [Online]. Available: https://www.ptcog.ch/archive/patient_statistics/Patientstatistics-updateDec2015.pdf. [Accessed November 2016].

[34] G. Lönn, "In-beam proton range monitoring during proton therapy," KTH Royal Institute of Technology, Stockholm, Sweden, 2016.

[35] H. Paganetti, Series in Medical Physics and Biomedical Engineering: Proton Therapy Physics, CRC Press, 2011.

[36] T. F. De Laney and H. M. Kooy, Proton and Charged Particle Radiotherapy, Lippincott Williams & Wilkins, 2008.

[37] W. D. Newhauser and R. Zhang, "The physics of proton therapy," *Physics in Medicine and Biology*, 21 April 2015.

[38] C. S. Chung, T. I. Yock, K. Nelson, Y. Xu, N. L. Keating and N. J. Tarbell, "Incidence of second malignancies among patients treated with proton versus photon radiation," *Radiation Oncology Physics,* vol. 87, pp. 46 - 52, 2013.

[39] M. W. Charles, "ICRP Publication 103: Recommendations of the ICRP," *Radiation Protection Dosimetry,* vol. 129, no. 4, pp. 500-507, 2008.

[40] V. Lobo, A. Patil, A. Phatak and N. Chandra, Free Radicals, antioxidants and functional foods: Impact on human health.

[41] M. J. N. Junk, "Assessing the Functional Structure of Molecular Transporters by EPR Spectroscopy," Springer Thesis, Berlin, 2012.

[42] J. A. Weil and J. R. Bolton, Electron Paramagnetic Resonance: Elementary Theory and Practical Applications, 2 ed., Hoboken, New Jersey: John Wiley & Sons, 2007.

[43] J. Jiang and R. T. Weber, ELEXSYS E 500 User's Manual: Basic Operations, Billerica: Bruker BioSpin Corporation, 2001.

[44] D. A. Schauer, A. Iwasaki, A. A. Romanyukha, H. M. Swartz and S. Onori, "Electron Paramagnetic Resonance (EPR) in Medical Dosimetry," *Radiation Measurements,* vol. 41, pp. 117-123, 2007.

[45] E. Adolfsson, Å. C. Tedgren, G. A. Carlsson, H. Gustafsson and E. Lund, "Optimization of an EPR dosimetry system for robust and high precision dosimetry," *Radiation Measurements,* vol. 70, pp. 21-28, 2014.

[46] H. Gustafsson, "Development of Sensitive EPR Dosimetry Methods," Linköping University Medical Dissertations, Linköping, 2008.

[47] E. Adolfsson, M. Karlsson, G. A. Carlsson, Å. C. Tedgren, E. Lund, S. Olsson and H. Gustafsson, "Investigation of signal fading in lithium formate EPR dosimeters using a new sensitive method," *Physics in Medicine and Biology*, vol. 57, pp. 2209-2217, 2012.

[48] Nuclear Power, "Nuclear Power," [Online]. Available: http://www.nuclear-power.net/nuclear-power/reactor-physics/interaction-radiation-matter/interaction-gamma-radiation-matter/#prettyPhoto. [Accessed February 2017].

[49] T. Inaniwa, N. Kanematsu, S. Sato and R. Kohno, "A dose calculation algorithm with correction for proton-nucleus interactions in non-water materials for proton radiotherapy treatment planning," *Physics in Medicine and Biology*, vol. 61, pp. 67-89, 2016.

[50] ETH Zürich, "ETH Zürich," [Online]. Available: http://www.epr.ethz.ch/education/basic-concepts-of-epr/one-elect--in-the-magn--field/zeeman.html. [Accessed November 2016].

[51] D. Wang, "Dovepress," vol. 8, pp. 439-446, 28 October 2015.

[52] Paul Scherrer Institut, "Paul Scherrer Institut," [Online]. Available: https://www.psi.ch/protontherapy/protons-and-their-properties. [Accessed November 2016].